Chapter 5 Results of the Geological Survey

5.1 Overview

The survey area is located between 10° and 12° S latitude (approximately 220km wide) and between 30° 30’ and 31° 00’ E longitude (approximately 55km long). The area is assigned to four 1/100,000 topological map sheets (1030NE, 1030SE, 1130NE, and 1130SE). The location of the survey area is shown by the blue square in Fig. 5.1.1.

Area for 100,000 scale geological mapping and survey
East longitude: 30° 30’～31° 00’, South latitude: 10° 00’～12° 00’ Area: No. 1030NE, 1030SE, 1130NE, 1130SE (East west: about 55km*South north: about 220km,

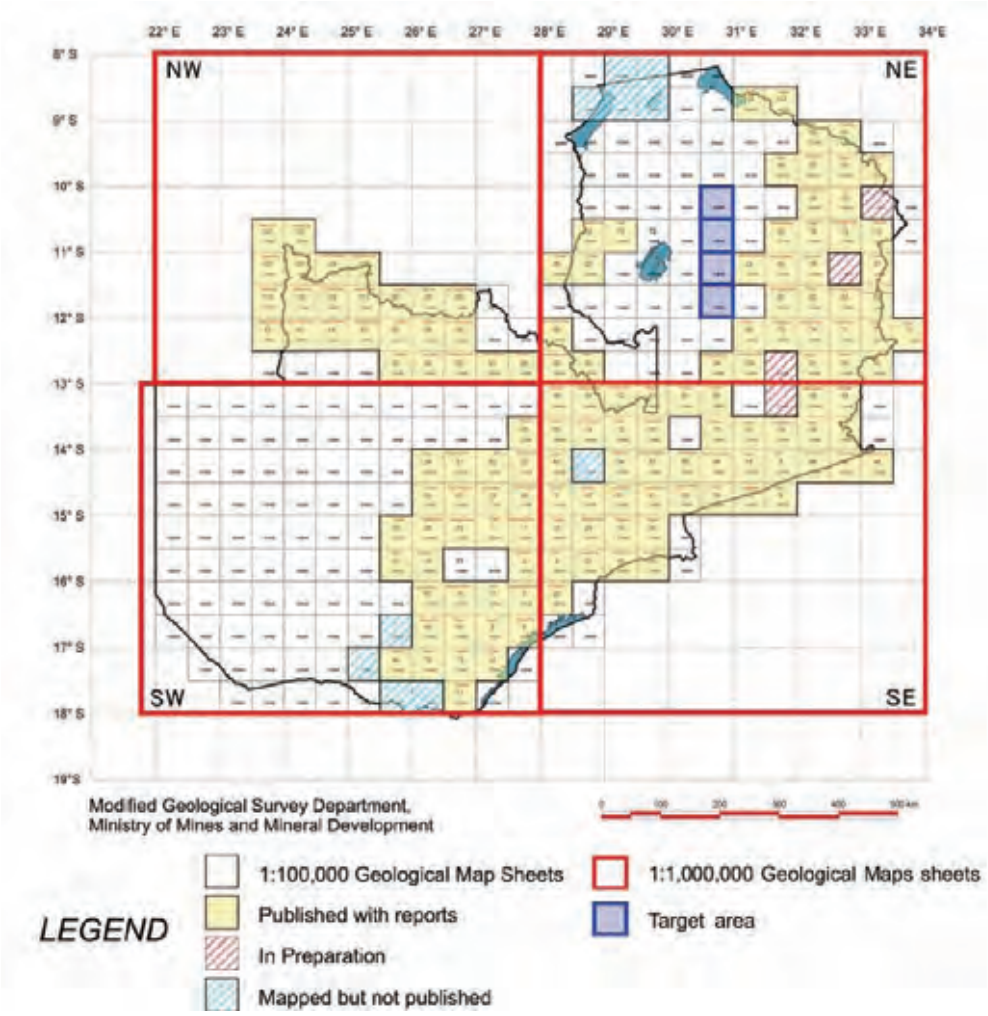

Fig.5.1.1 Survey Area

The geologic field surveys were designed to create 1/100,000 geological maps and to provide information on mineral resource potential to contribute to investment promotion. These surveys have included the preliminary geological survey (the first site study in February, 2007), reconnaissance geological survey (the second site study in June and July, 2007) and detailed geological survey (the

second site study (2) from August to November, 2007, and the third site study from July to October, 2008). Table 5.1.1 shows the research objectives and survey contents at each stage.

Table 5.1.1 Contents of Each Geological Survey

Survey stage	Main target area	Purpose	Contents
Preliminary survey (Feb. 2007)	・All four sheets	・To understand the geography, geology, access of all target areas	・Confirm access to main highways, outcrop, public safety, village conditions, etc.
Reconnaissance Survey (Jun. to Jul. 2007)	・All four sheets	・To understand the geography, geology, access of all target areas	・Confirm access to main highways, outcrop, public safety, village conditions, etc. ・Investigate a preliminary pit
Geological Survey (Aug. to Nov. 2007)	・Sheet No.1030NE and 1030SE	・1/100,000 geological mapping ・To understand the mineral resource potential	・1:50,000 geological route survey, creation of a route map ・Stream sediments geochemical survey ・Take samples for lab tests ・Pit surveys
Geological Survey (Jul. to Oct. 2008)	・Sheet No.1130NE and 1130SE	・1/100,000 geological mapping ・To understand the mineral resource potential ・Follow-up of all study areas	・1:50,000 geological route survey, creation of a route map ・Soil geochemical survey ・Take samples for lab tests ・Pit surveys ・Flow up surveys of all target areas

5.2 Results of the Surveys

5.2.1 Satellite Image Analysis and Results of the Preliminary Survey

Most of the survey area is covered with vegetation and a thick weathering layer, so areas of exposed rock are very limited. For efficient survey design, it is important to know where outcrops are likely to occur before undertaking the site work. Possible outcrops were estimated by analyzing satellite images such as multi-shading images of SRTM/DEM (Fig. 5.2.1) and ASTER false color images (Fig. 5.2.2). A ground truth survey was carried out to verify the analysis. Possible outcrops were accessed using a handheld GPS receiver.

The results of satellite image analysis are summarized as follows:

•Topographical features in the southern part of the survey area (sheet 1030SE, 1130NE, 1130SE) show a flat plain where relief is extremely low, though drainage systems are somewhat developed in the northern part (sheet 1030NE, Fig. 5.2.1). According to previous 1:1,000,000 geologic maps, the geological structure of the northern part of the area consists mainly of granitoids and metasediments. Sedimentary rocks and alluvium are distributed widely in the southern part of the area.

•Special attention was paid to ridges or cliffs represented by high contrast color in the multi-shading images, because outcrops generally tend to appear in the steep slopes and cliffs of a river valley. When blue to white color in the ASTER image coincided with a ridge or cliff in the multi-shading image, it was identified as a “possible outcrop” (Appendix V-1). In the preliminary survey, site

verifications using GPS were conducted on two identified points (outcrops No.1 and No.6 in Fig. 5.2.1 and 5.2.2) that were adjacent to the main road and which were confirmed by the ASTER images.

•The two "possible outcrops" were confirmed as "substantial outcrops" of quartzite by this ground truth survey.

>Outcrop No.1: boulders of massive pale pink quartzite of 3×4m or less in size scattered among about 3m high scrub.

>Outcrop No.6: boulders of massive white quartzite of 1.5×2m or less in size scattered among 3-4m high scrub.

Besides the above-mentioned two outcrops, four other outcrops (No.2 - No.5) were detected as shown in Table 5.2.1 and Appendix V-2.

Table 5.2.1 Results of Outcrop Observations in the Preliminary Survey

Outcrop No.	UTM coordinate		Rock name	Color	Minerals	Grain size	Shape of mineral	Remarks
	X	Y						
1	263093	8855900	Quartzite	light pink	qz>>flds,hem /mt?	medium>> coarse	Sub-angular /Sub-rounded	tabular big boulder (max 3x4m), bedding
2	265167	8853026	Quartzite	light pink	qz>>flds,hem /mt?	medium>> coarse	sub-angular	float?
3	263215	8855636	Quartzite	light pink	qz>>flds,hem /mt?	medium>> coarse	sub-angular	bedding structure (NW27/35E,
4	263112	8856092	Quartzite	light pink	qz>>flds,hem /mt?	medium>> coarse	Sub-angular /Sub-rounded	tabular big boulder (3x20m)
5	264439	8887276	Quartzite, shale, ferruginous rock	(Quartzite) white-light gray, (shale) light yellow	(Quartzite) qz>>flds?	medium>> coarse	sub-angular (Quartzite)	bedding structure (shale)EW-NE75/20-24S
6	268659	8883564	Quartzite	white-light gray	qz>>flds,hem /mt?	medium>> coarse	sub-angular	tabular big boulder (max

qz:quartz, flds:feldspar, hem:hematite, mt:magnetite

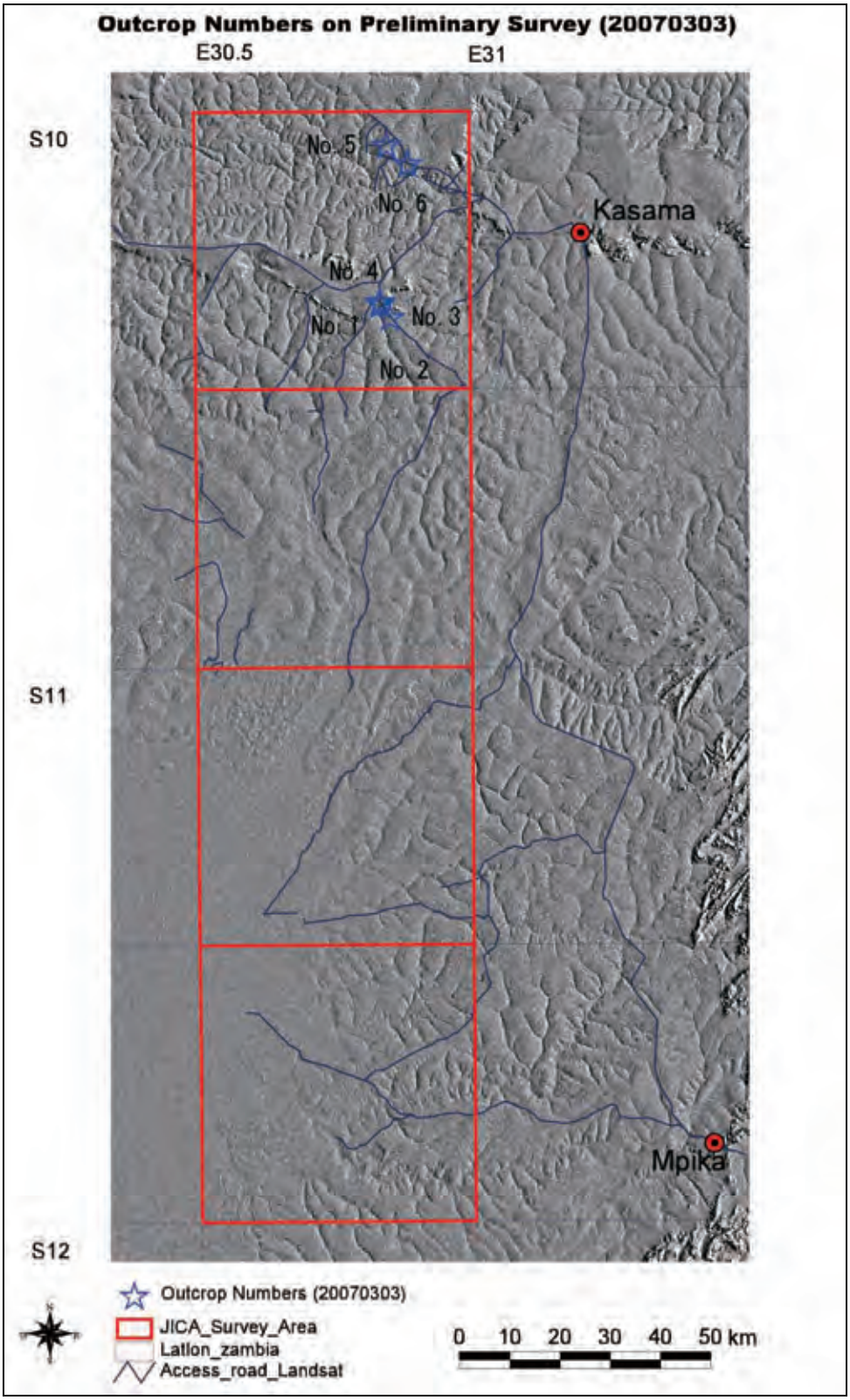

Fig. 5.2.1 Multi-Shading Images and Locations of Outcrops

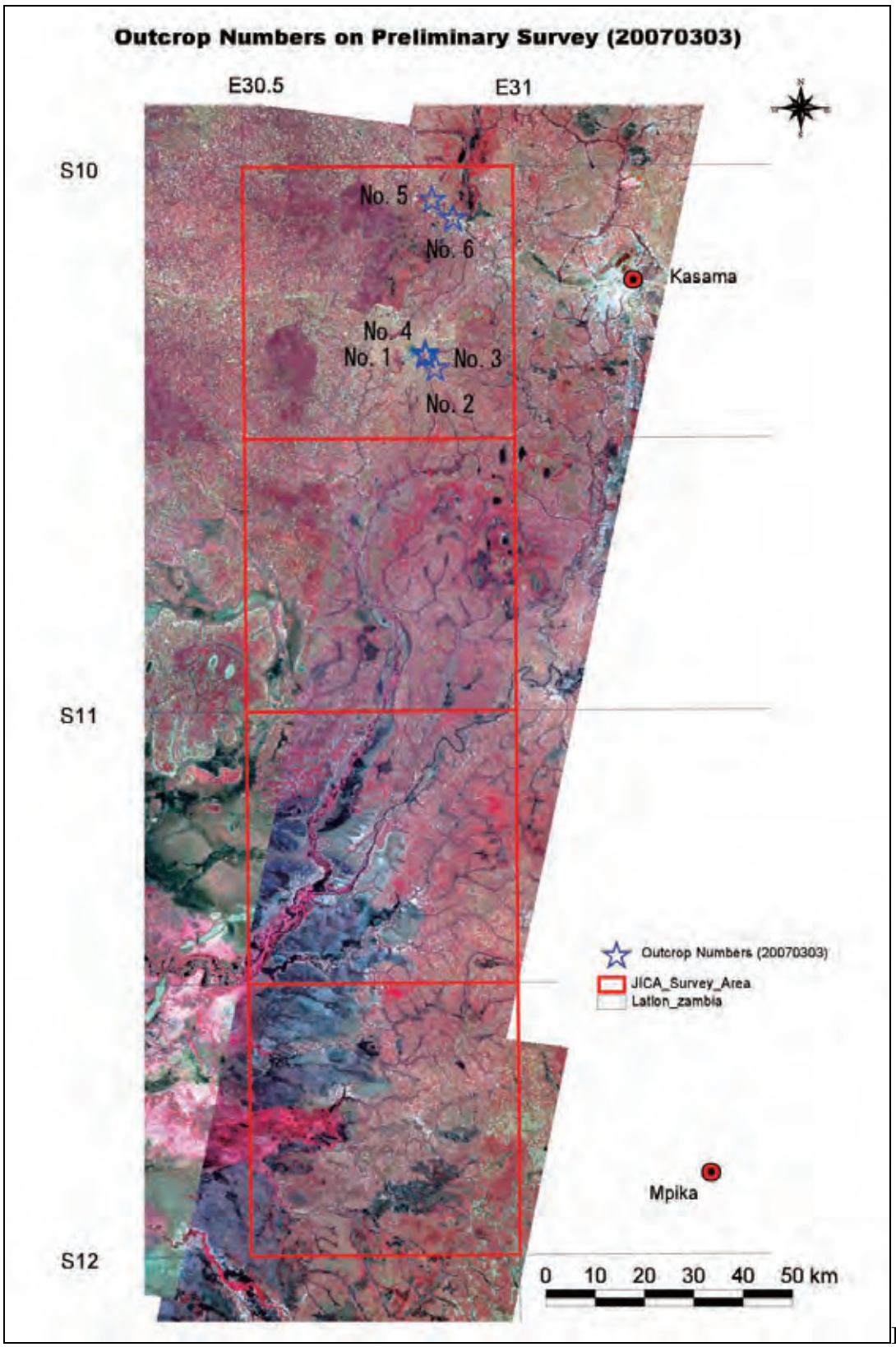

Fig.

Fig. 5.2.2 ASTER False Color Imagery

5.2.2 Results of the Reconnaissance Survey

In the reconnaissance survey, general information on the entire survey area was collected to conduct the subsequent detailed geological survey more effectively. The state of outcrops, sampling points, and a candidate base camp site were investigated. Preliminary check pits were excavated. The reconnaissance survey was mainly implemented along vehicle-accessible roads. The surveyed route for the reconnaissance survey is shown in Fig. 5.2.3.

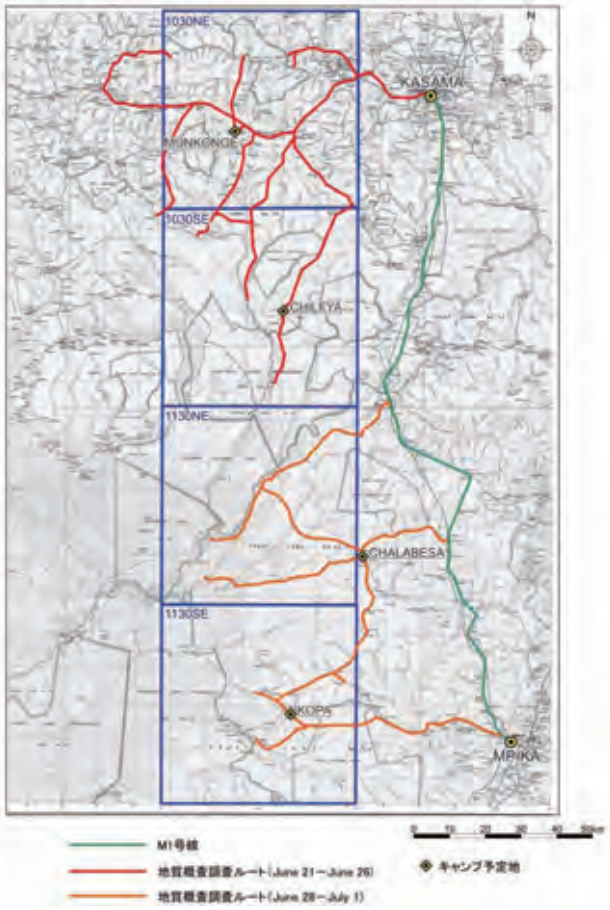

According to the previous 1:1,000,000 geological maps, the survey area is composed of 1) basement complex, 2) Muva Supergroup, 3) Katanga Supergroup, and 4) alluvium. The surface of the survey area has widely been affected by lateritic weathering. To observe rock facies and their geological structure, site observations were conducted in the following 25 places (Appendix V-3 and V-4):

i) Basement Complex: 2 places
ii) Muva Supergroup: 4 places
iii) Katanga Supergroup : 4 places
iv) Alluvium and weathered layer: 6 places
v) Float: 9 points

In the survey, neither mineralization nor alteration was detected.

Fig. 5.2.3 Reconnaissance Survey Route

(1) Basement Complex

Approximately 5m×10m outcrops of the Basement Complex were found in the Mukanga River in the northern part of the 1030SE map sheet (Photo 1 in Appendix V-5). They consisted of pale greenish and homogenious holocrystalline granites, composed of mainly plagioclase containing quartz and potash-feldspar (Lh7062201). The mafic minerals were mostly biotite, with some pale greenish epidote. Moreover, 3×5m granite outcrops (Lh7062502_1; Photo 2 in Appendix V-5) with similar rock facies were exposed about 2km west of the Lubansenshi River in the central part of the 1030SE map sheet. Pegmatite (Lh7062502_2) composed of quartz and feldspar of about 80cm in length and 40cm in width was found at the east end of the granite outcrop. Because the boundary between granites and pegmatite is indistinct, the intrusive relation between the two rock types is

uncertain. However, it is thought that the pegmatite might be a part of the quartz and potash-feldspar veins which penetrate the granites because several quartz and potash-feldspar veins oriented N70°W were found in the outcrop. A thin conglomerate layer (<1cm, Lh7062502_3; Photo 1 in Appendix V-5) containing quartz grains (1.5cm or less) is scattered in the central part of the outcrop (Photo 2 in Appendix V-5). The conglomerate layer overlies the granite horizontally.

(2) Muva Supergroup

The outcrops of the Muva Supergroup were confirmed in four places in the 1030NE map sheet. They all consist of quartzite, which is divided into the following three types:

i) Massive white quartzite which is slightly exposed in the northeastern part of the 1030NE map sheet. It consists of coarse quartz gains of 2mm or less (Lh7062407-2). Moreover, a layer (Lh7062407-1) of fine-grained black minerals similar to hematite was found in the outcrop with striking N30°W and dipping 30°NE (photo 3 in Appendix V-5)). Layers of quartz grain concentration, which are very porous, have developed in the outcrop.

ii) Pale pink quartzite which extends from east to west in the central part of the 1030NE map sheet area. This quartzite consists of fine quartz grains and is harder than the quartzite mentioned above. The black minerals layer is thinly intercalated, striking E-W, dipping 30°S (photo 4 in Appendix V-5).

iii) Grayish white quartzite including fine-grained biotite is exposed in 5x10m outcrops along the Kapulu River in the northwestern part of the 1030NE map sheet area. This type quartzite is characterized by a strongly folded structure: the direction of the fold axis in this outcropping is roughly N50°- 60°W (photo 5 in Appendix V-5).

(3) Katanga Supergroup

The Katanga Supergroup was confirmed at four places in the map sheets of 1130NE and 1130SE. It is composed of quartzite, sandstone and siltstone. Quartzite of the Katanga Supergroup shows weaker re-crystallization than that of the Muva Supergroup. The quartzite is accompanied by white fine clay in matrix. The quartzite dips gently to the north or northeast (striking N78°E with dipping 4°N at Lh7063002, and striking N55°E with dipping 8°NW at Lh7062801; Photo 6 and 7 in Appendix V-5). N40E oriented fractures have partially developed (Photo 6). In addition, re-crystallized quartz grains concentrating in layers of 3mm or less in thickness occur with the quartzite. Yellowish ochre to light green colored siltstone is exposed in approximately 1x2m outcrops in the Luitikila River in the southern part of the 1130SE map sheet area. This generally indicates fine-grained, massive and soft lithofacies.

(4) Weathered layer

A weathered layer covers most of the survey area, especially in the 1130NE and 1130SE sheets. Several pit excavations showed the thickness of these formations to be at least 4m.

(5) Floats

Observations of float boulders were conducted to supplement the limited geological information resulting from the poor rock exposure of the survey area. The floats consist mainly of granitoids and quartzite. Dark grey to dark greenish dolerite boulders (60cm x 1m; Lh7062602) were detected 2km west of the western central margin of the 1030NE map sheet area. Drusey vein quartz floats are scattered in the eastern part of the 1030SE sheet area. It is assumed that dolerite dykes, quartz veins and pegmatites are exposed in the survey area, although the source outcrops of these floats could not be ascertained.

5.2.3 Results of the detailed geological survey

Based on the results of the preliminary and reconnaissance surveys, the geological survey and sample collecting were conducted along main streams and ridges. Existing 1:250,000 and 1: 50,000 topographic maps and ASTER and SRTM/TM satellite imagery were utilized for this field work. Survey routes were designed by considering geologic features such as stratigraphy, faults and folding on the 1:1,000,000 geological map and access information derived from satellite image analysis. The results of the field observation are described in the field notes, and in the field observation sheet (Appendix V-6).

Accurate coordinates of all the outcrops and sampling points were recorded using a handheld GPS receiver (map datum ARC1950 and WGS84). Also, observed geological information was compiled on a 1/50,000 route map. The geologic features of rock occurrence and mineralization of important outcrops were observed in detail, and they were recorded on sketches and photographs. The survey results were summarized in the route maps and 1:50,000 geological maps.

Generally in Zambia, major district toponymies put as 1:100,000 geological map names published in Zambia. In this study, four sheets of 1030NE, 1030SE, 1130NE and 1130SE were named ”Chishimba Falls Area”, ”Chilufya Area”, ”Mbati Area”, and ”Kopa Area”, respectively.

5.2.3.1 Stratigraphy

Each geological unit is named according to previous studies（e.g. 1:1,000,000 geologic map published by GSD, 1974; Daly and Unrug,1982）and the results of isotropic dating age from this study.

The schematic stratigraphic column and geological map are shown in Fig. 5.2.3.1-1 and 5.2.3.1-2. The results of petrographical observations and whole rock chemical analysis are shown in Appendix 7 and 8 respectively.

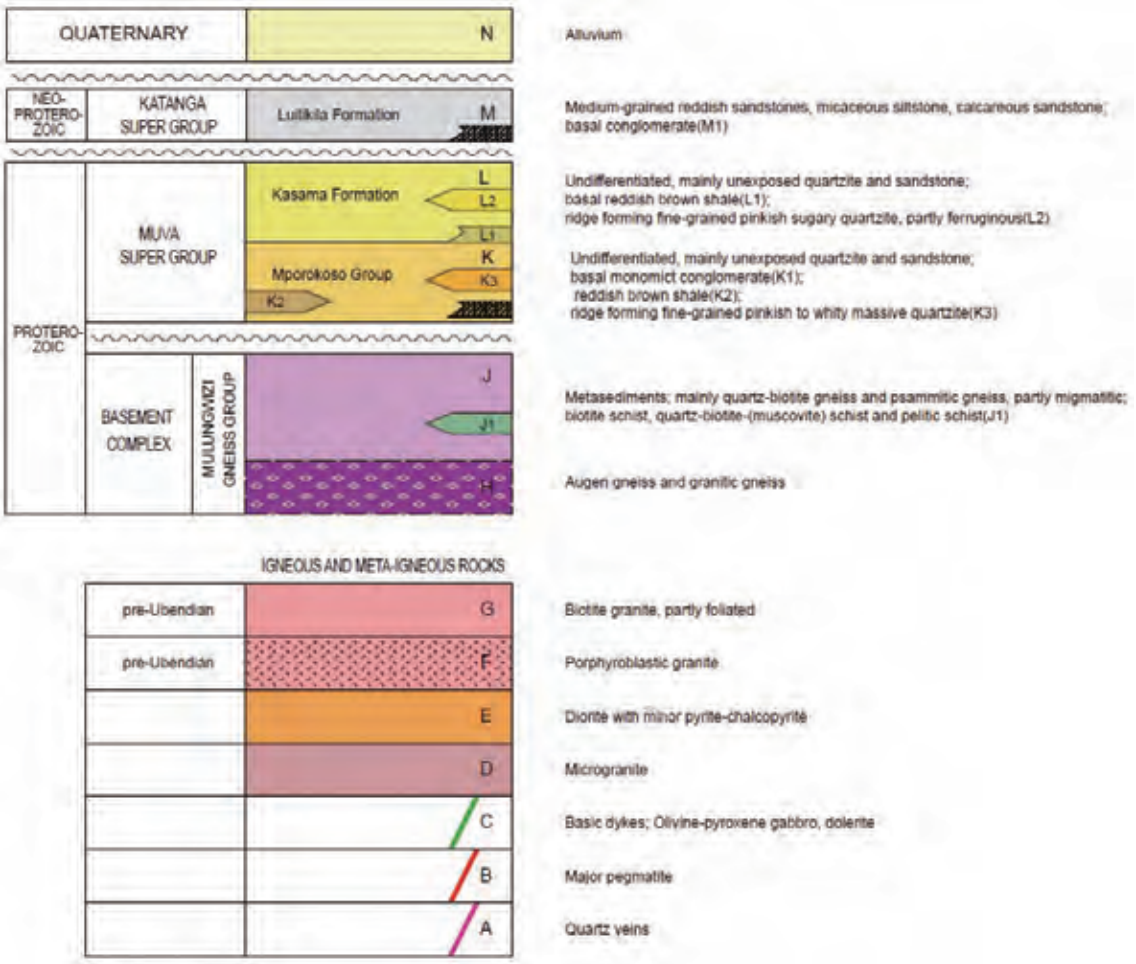

Fig. 5.2.3.1-1　Schematic Stratigraphic Column of the Survey Area

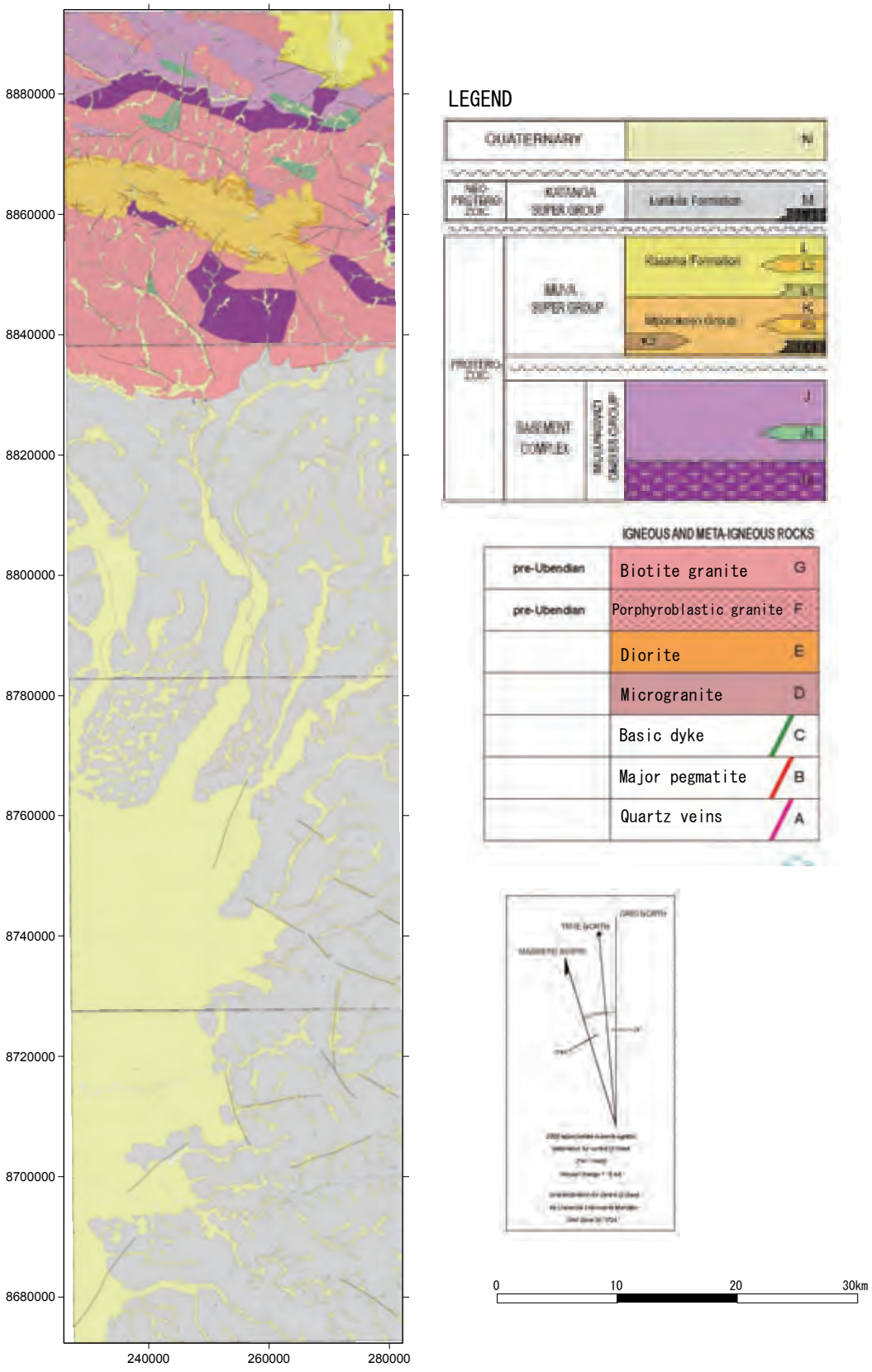

Fig. 5.2.3.1-2 Geologic Map of the Survey Area

The survey area is located in the southernl part of the Bangweulu block which is surrounded by the Ubendian belt, Irumide belt and Kibaran belt (Drysdall et al.,1972, Fig5.2.3.1-3). The Lower to Middle Proterozoic basement complex comprises granitic rock (Gr; granitoids, granitic gneiss) and metasediments (Bmq; psammitic gneiss, quartzite, sandstone, siltstone and muscovite schist). The basement complex is overlain by Middle to Upper Proterozoic sedimentary rocks (quartzite, sandstone, siltstone and schist) and alluvial cover. The basement complex is intruded by metavolcanics (Imv) and gabbros (Igb).

Mafic (gabbroic) composition intrusions occur in a mainly transitional zone between granitic rock and psammitic gneiss of the basement complex. Granodioritic intrusion occurs at the confluence of the Mwelekumbi and Lukulu rivers. Acidic metavolcanics accompanying quartz crystal occur in a small area of Mukanga and Likupa streams.

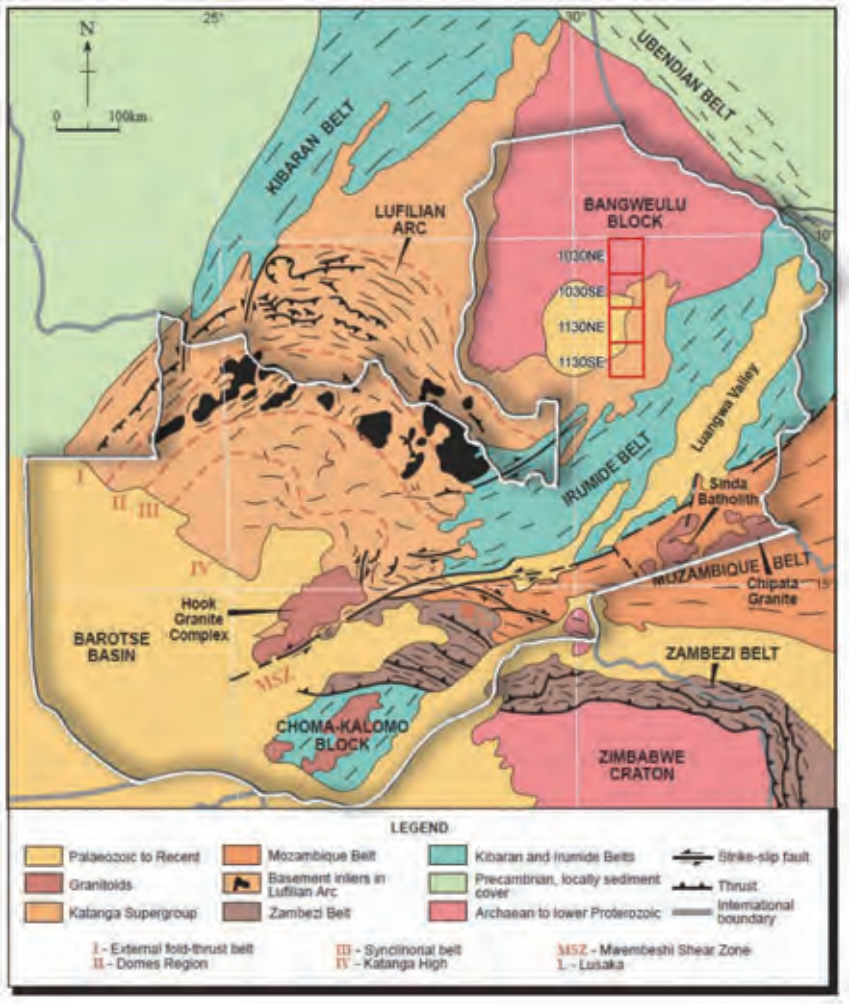

Fig. 5.2.3.1-3 Geological setting of the Survey Area Based on a Geologic Map of Southeast Africa(Goodwin, 1996)

1） Basement Complex

The basement complex occurs in the 1030NE sheet area and in the northern margin of the 1030SE sheet area. The basement complex comprises granitoids and metasediments accompanying pegmatites and quartz veins. Field observations indicate that the granitoids are divided into biotite granite, porphyroblastic granite and granitic gneiss. The metasediments comprise mainly psammitic schist and psammitic gneiss, and occasionally mica schist and biotite schist. Metasediments partly interlays sandstone, shale, and slate. The boundaries between granitoids and metasediments are characterized by a migmatitic structure.

(a) Granitoids

Biotite Granite

There are outcrops of granitic rocks in the 1030NE sheet area and in the northern margin of the 1030SE sheet area. Representative occurrences of this biotite granite have been found in the Mwelekumbi River, Lukulu River, Lubala River, Kapulu River， and Mukanga River

The granitoids in the area are leucocratic or pinkish to brownish in color. The size of phenocryst is 1 to 5 cm. The common mafic mineral of the granitoids is biotite, but occasionally hornblende (Fig.5.2.3.1-4）.

Fig. 5.2.3.1-4 Granitoids (left: Lh7100201; right: Lh7091203)

Outcrops of the light grayish granite (LI07100803: 270354 8851771) occur in the Mwilondwe River in the southeastern part of 1030NE. The granite has phenocrysts of 1 to 2 mm and a holocrystalline texture. Naked eye observation indicates that colored minerals occupy up to 25% volume .

Outcrops of the grayish granite (Pg62: 279149 8857090) occur in the Lukulu River in the southeastern part of 1030NE. The granite has coarse phenocrysts and a porphyritic texture. Naked eye observation indicates that biotite with epidote occupy up to 25% volume.

Outcrops of the grayish granite (FC091929: 244690 8868852) with weak foliation occur in the Kakondokwa River in the central part of 1030NE.

Leucocratic and relatively coarse biotite granite (Pg70: 249107 8829974) occurs in the northern area

of 1030SE. Naked eye observation indicates that dark greenish gneissose granite (Pg59:226527 8837232) with weak foliation contains up to 20% biotite. Some of the biotite has turned into epidote. Biotite granite sometimes has a weak foliation structure. It is impossible to observe direct relations between biotite granite and granitic gneiss because there is no outcrop showing contact of both rocks. Transitional changes from biotite granite to gneissose granite and granitic gneiss would be estimated according to metamorphism.

Porphyroblastic granite

Granites with porphyroblastic textures characterized by large potash feldspar are quite common in the Nsamba River, Samba-Lubemba River, and Samba-Bemba River. Potash feldspar phenocrysts up to 5cm in representative occurrence (Lh7100502: 261910 8888928） are grayish white or pink in color and define a penetrative mineral lineation concordant to the regional structural trend of 110° to 120° (Fig. 5.2.3.2-5).

The porphyroblastic granite includes xenoliths of psammitic schist around the boundary between this rock and metasediments. The xenoliths of gray pale metasediments of 20 to 50 cm in size or dark brown gneiss in porphyroblastic granite (Fig.5.2.3.1-6) have been observed in the Samba-Lubemba River (Lh7100208: 258874 8888474) and the Samba-Bemba River (Lh7100504: 259872 8887646）.

Fig. 5.2.3.1-5 Foliated Porphyroblastic Structure in Granitic-gneiss (left: Lh7100503; right: Lh7091804)

Fig.5.2.3.1-6 Rock Fragments in Granitoids (Lh7100503）

Granitic gneiss and augen gneiss

Granitic gneiss is distributed in zonation around the boundary with metasediments in northern area. In southern area, granitic gneiss in Mwilondwi River, Mwefu River, Nsontola River, and Mungombe River shows augen gneiss structure.

Granitic gneiss is generally composed of medium to coarse quartz, feldspar and biotite. Lineation of porphyritic phenocryst shows WNW-ESE trend (mostly N60°-80°W). An augen structure characterized by a concentration of ellipse crystals of potash feldspar up to 3 cm was observed in the Mwefu River (Lh07101502: 260114 8839049）.

Migmatite

Migmatite has two types: one with granitoids dominant and the other with metasediments dominant. Granitoids-dominant migmatite (N091602: 260668 8863176)includes large xenoliths of metasediments elongated along the direction of schistosity (Fig. 5.2.3.1-7). Granite in migmatite has weak foliation. The boundary between granite and metasediments is clear.

In the case of metasediments-dominant migmatite, metasediments sometimes include thin granite layers or lenses of granite.

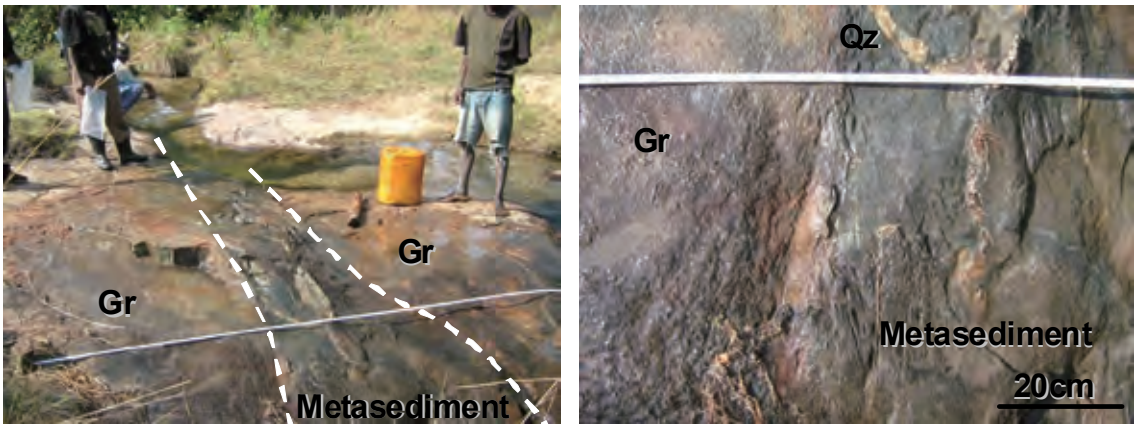

Fig. 5.2.3.1-7　Outcrop of Migmatite (N091602）

（b）Metasediments

Metasediments comprise mainly psammitic schist, psammitic gneiss accompanied with biotite schist and slate, sandstone. The metasediments occur in the north-western and north-eastern parts of the 1030NE sheet area. It forms a metamorphic belt oriented WNW-ESE. Some of the metasediments are penetrated by irregularly-shaped migmatite.

Psammitic schist (siliceous schist and quartz schist）

Psammitic schist comprises mainly fine-grained quartz accompanied by a small amount of fine (<1mm） feldspar and biotite. Bedding structures are observed in some places, although massive texture is predominant in psammitic schist. The dipping is generally steep and the rocks are folded

on a northwest axis. Thin layers of slate or shale are interlaid in psammitic schist.

Muscovite crystals in 3 to 5 mm in size with ellipse or spherical shape were observed in psammitic schist (Lh7091205: 237254 8892726)in Mukalamba River, northwestern part of 1030NE(Fig.5.2.3.1-8 left). The fine grained psammitic schist (N091502: 260,920 8,885,626) outcrops in Mukoba River in northeastern part of 1030NE. It is light gray in color, hard, and massive with a banded structure that is not clear. Biotite in this rock is less than 0.5mm in size and has foliation. Psammitic schist is cut by quartz-biotite veinlets.

Fig.5.2.3.1-8 Foliated Recrystallized Muscovite in Massive Psammitic Schist (left: Lh7091205) and Psammitic schist with veins (right: N091502）

Psammitic gneiss

Psammitic gneiss is distributed in the Samba-Lubemba River, Nsamba River, and Samba-Bemba River in the northeastern part of 1030NE, and partly in the Kapalu River in the northwestern part. Psammitic gneiss is composed mainly of medium-grained quartz accompanying feldspar and fine biotite.

Psammitic gneiss in the Samba-Lubemba River, Nsamba River, and Samba-Bemba has weak micro-folded structure with a general WNW-ESE trend of schistosity. Dips show vertical or dipping 70°S. The boundary between this rock and porphyroblastic granite is not clear. The boundary is characterized by a migmatitic structure showing irregular granite mixing in psammitic gneiss.

Light gray psammitic gneiss occurring in the Kapala River (Lh7062605: 228,108 8,881,636)has a typical gneissose banded texture with microfolds. Light gray psammitic gneiss (N091707: 228,2058,881,114)with complicated microfolds comprising quartz, feldspar, and minor biotite of less than 1% vol.

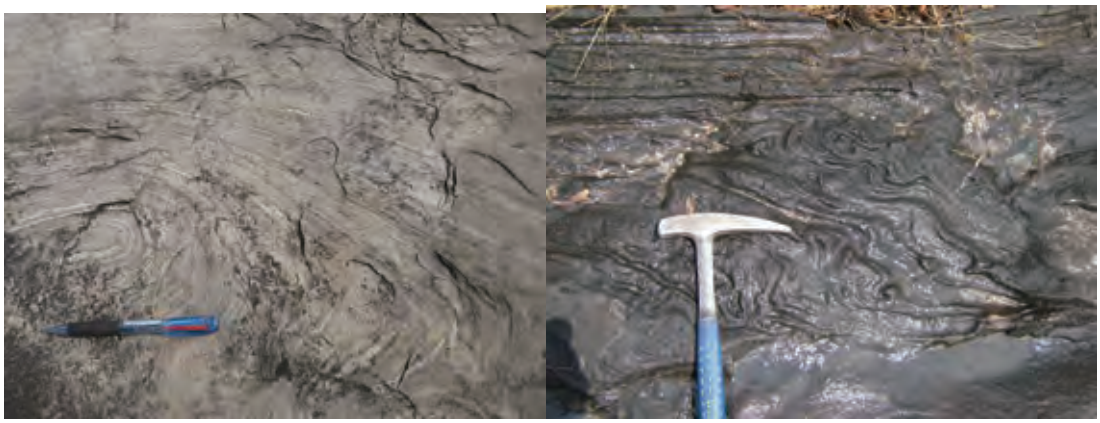

Fig 5.2.3.1-9　Psammitic Gneiss with Microfolds (Left:Lh7062605 Right:N091707）

Biotite gneiss – biotite schist

Fine biotite gneiss occurs in the Nkanga River (N091603: 260,286 8,863,668) in the northeastern part of 1030NE (Fig. 5.2.3.1-10). Biotite gneiss is dark gray in color, hard, rich in biotite, and has a clear banded structure. The macro trend of schistosity shows a N55°W strike though gneiss was deformed with microfolds. Dipping is almost vertical. In this outcrop, biotite gneiss sometimes includes thin layers or lenses of granite.

Fig. 5.2.3.1-10 Outcrop of Biotite gneiss and Microfolds(N91603）

Biotite schist is exposed along the Nkanga River (Lh7110603: 260018 8863743）. It is characterized by abundant (>50%） fine (<1mm） biotite accompanying quartz, plagioclase, muscovite and potash feldspar. Its schistosity is dipping 70°eastward, and a northeast (44°） strike which goes against the general structural trend of this area (WNW-ESE strike, steeply dipping southward)

A fine light gray biotite gneiss in the Nkanga River (N091607: 259,325 8,862,116)was penetrated by pegmatite. Plagioclase in gneiss was turned into potash feldspar around the boundary of pegmatite.

Mica schist

In the 1030NE sheet area, mica schist is exposed in small outcrops along the Luluku and Nkanga rivers. Along the Luluku River, grayish to light yellow fine (<1mm) muscovite schist is exposed with a strike of 290° to 300°, dipping 70° to the vertical with clear schistosity (Fig. 5.2.3.1-11).

Fig 5.2.3.1-11 Muscovite schist (Lh7100103)

Outcrops of highly weathered brownish mica schist (M34: 265552 8867708) occur in the Nkanga River. Clear schistosity showing an E-W strike and dipping 60°N has been observed though the rock has been severely weathered.

Sandstone

Outcrops of jointed sandstone (N091311: 279,240 8,879,860)5m width in Lukupa River, northeastern part of 1030NE. It is light yellowish green in color and has clastics in 0.1-0.5mm.

2) Muva Supergroup

The Muva Supergroup exposed in this area is subdivided into the Mporokoso Group and the Kasama Formation. The Mporokoso Group comprises sedimentary sequences of quartzites and is part of what was formerly called the 'Plateau Series' (Guernsey 1941). Unrug (1982) divided the Plateau Series into two lithostratigraphic units of the older Mporokoso Group and the younger Kasama Formation. This sedimentary cover of the former Plateau Series underlies an area of approximately 41,000 km2 in the northern parts of Luapula and Northern provinces (Thiemes, 1971) and extends into Katanga Province of the Democratic Republic of Congo. The succession was regarded to be part of Upper Kundelungu by Robert (1940), though Phillips (1955) considered it to be a transgressive end-stage of Muva deposition. De Waele and Fitzsimons (2004) estimated that sedimentation of the Mporokoso Formation started in 1.86 Ga based on the results of zircon SHRIMP (U-Pb） dating of Mporokoso quartzite sampled in the Mansa district (west of the survey area）, but isotropic dating ages of the Mporokoso Formation and Kasama Formation have not been reported in the survey area.

(a) Mporokoso Group

The Mporokoso Group is exposed from the western part (Mumana Lupando） to the eastern part (Dominiko） of the survey area. It shows a gentle syncline which extends along a W – E or WNW – ESE trend axis. The Mporokoso Group may unconformly overlie the basement complex based on their respective lithofacies and structural relationship, although direct contact between them has not been observed.

The Mporokoso Group comprises mainly gray to grayish brown massive quartzite. Locally, well-rounded quartzose monomictic conglomerates have developed in the basal horizon of this group. A few meters of brown or light purple shale are occasionally interbedded in the quartzite.

Quartzite

Quartz grains are fine to medium (<3mm）. Quartzite gently dips up to 15° around the Mukanga River (western part of the 1030NE sheet area）, whereas it shows rather steep dipping of 40° to 60° around the Lubala River (northern part of the 1030NE sheet area）. The quartzite is mostly ridge-forming outcrops in the central area of the sheet. It is pink to purple and largely medium-grained but coarsens downwards. The quartzite is poorly sorted and graded bedding occurs in places. Constituent grains range in size from 0.5 to 3cm and they are semi-angular to rounded. The rock is grain-supported and has silica as the main cementing material, making the quartzite well cemented.

Cross bedding (Lh7090704: 235342 8861290） is observed in outcrops of the upper reaches of the Mukanga River (Fig. 5.2.3.1-12, left）. It accompanies an “en echelon” fractured quartz vein (Fig.5.2.3.1-12, right）. Sykes (1995） reported this as a common feature of the Mporokoso Group in the Chilipi area which is located in the south-western part of the survey area. But polymictic basal conglomerates predominate in the Chilipi area.

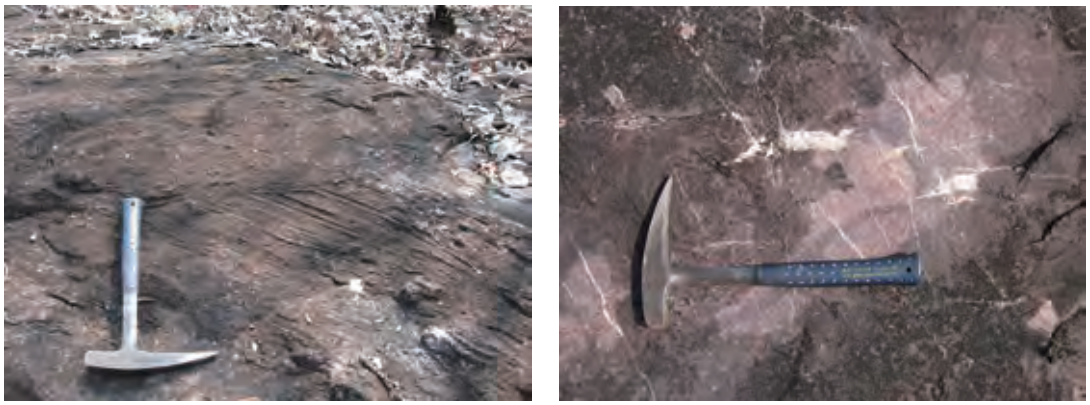

Fig. 5.2.3.1-12 Cross -lamination Structure of the Mporokoso Group (Left: Lh7090704）, Sigmoidal and en Echelon Fractures (Right: Lh7090706)

Pink to light purplish quartzite (N091301: 263394 8860614) is exposed near Dominiko Village. Quartzite composed of abundant quartz grains of 0.3-0.5mm in diameter shows a granoblastic texture by recrystallization. This quartzite is rich in silica, 96.9% SiO_2.

Conglomerate

The basal conglomerate rarely outcrops, and was observed just in two places in 1030NE.

The basal conglomerate in the upper reaches of the Mukanga River (Lh7090708:235984 8862029) comprises well-rounded quartz pebbles. It is characterized by monomictic features, poor sorting and a white or light brown color.

The large float in 1m size of light pinkish colored basal conglomerate in the upper reaches of the Futaba River (N091606: 256353 8864370) comprises sub-rounded quartz pebbles of 1 to 2 cm. Clast occupies 50% vol, matrix comprises fine quartz. No dipping or strike was observed due to floats.

Fig. 5.2.3.1-13 Conglomerate of the Mporokoso Formation (N091606)

Shale

Shale is generally brownish to light purplish in color. It is interbedded in quartzite of several meters in thickness. The shale has sharp boundaries with the quartzite. Highly weathered shale (M52: 253859 8857875) was observed at the quarry for road construction. Due to its softness and easily weathered character, exposure is limited to the flanks of ridges, road cuts, laterite quarries and stream channels.

(b) Kasama Formation

The Kasama Formation extends from around the Luombe River to Chishimba Falls (in the north-eastern part of the 1030NE sheet area). Drysdall (1960) reported unconformity contact of Kasama Formation quartzite with basement siltstone discovered during excavation for the Chishimba Falls electric power plant.

The Kasama Formation extends 100km from the north-eastern part of the 1030NE sheet area to Chapalapata Hill, which is located west of Isoka town (Daly and Unrug, 1982). The thickness of the

group ranges from 900m in the eastern part to 100m in the survey area. Type locality of this group occurs in Mabula (12km west of Kasama） where the 120m thick group is divided into four units.

Quartzite

The Kasama Formation comprises mainly whitish or pinkish quartzite with interbedded light purplish shale. Typical occurrences can be observed at Chishimba Falls. The Kasama Formation shows generally gentle dipping.

The quartzite shows a massive texture and consists mainly of fine to medium size (max 3mm） quartz grains. It is characterized by a well-sorted texture of sugary quartz crystals. Beddings or laminations which accompany black-colored, fine thin layers of hematite are often observed.

A continuous shear zone in quartzite (N091501:26288 8886936) is found in the E-W direction along the stream.

Light pink colored fine quartzite (N091505: 26259 8886747)shows a 50°E strike and 24°SE dipping. Chemical assay results indicate high quality silica, 98.4% of SiO_2.

Shale

Shale occurs not only in the basal part, but is also interbedded in layers of 1-2 meters thickness in quartzite. The shale (N091316: 272293 8881446)is generally yellowish white in color due to weathering, but is brownish in the iron-rich part. Bedding strikes N30°W and dips 8°NE.

Pinkish shale occurring in the bottom of the quarry (N091506: 264429 8887556) shows a gentle dip of 3°SW

3) Katanga Supergroup

(a) Luitikila Formation

The type locality of the Luitikila Formation is the Luitikila River which is located northwest of Mpika town (Guernsey, 1941）. The Luitikila Formation of the Chalabesa Mission sheet (1131NW） area comprises sandstone, siltstone and mudstone (Martin, 1968）. It unconformly overlies the Mansha River Group (a part of the Muva Super Group）. A 50m thick bed of quartzitic conglomerate was reported at the base of the Formation.

The Luitikila Formation occurs in the 1030SE, 1130NE and 1130SE sheets of the survey area. Fresh outcrops of this Formation are very rare because it has generally been subjected to strong lateritic weathering.

-1030SE Sheet

Fine sandstone and siltstone

The Luitikila Formation comprises brown or light brown colored fine sandstone to siltstone which

contains feldspar and fine-grained muscovite. Bedding structures are common and fine (<1mm) muscovites that have developed along irregular schistosity. Lamination of fine and black hematites is occasionally observed.

Three outcrops of the Luitikila Formation were observed along the Chambeshi River in the 1030SE sheet area. Each outcrop shows a NE-ENE strike and 2° to 8° gentle dipping. Thin (<3mm) hematite laminas without muscovite were observed in outcrops (Lh7103101: 280295 8790036), whereas 30m south of there, fine (<1mm) muscovites without hematite have developed. Some similar characteristics were observed in the outcrops along the Lubansenshi River. In the southern (downstream) reaches of the Lubansenshi River, outcrops of the Luitikila Formation comprise red bed sandstone with a 5mm hematite layer without muscovite (Lh7102601:256716 8797750).

No outcrops were found except around the Chambeshi River and Lubansenshi River due to the flat topography. The pebbles excavated from water wells in villages were examined to obtain covering geological information.

There is an unused water well of 20m in depth in a village near the Lukutu River (227526 8818186). Pebbles excavated from the deep part were pinkish in color, sandstone comprised of sub-angular quartz of 1cm in diameter and minor feldspar. It resembles sandstone from the Lubansenshi River. Reddish fine sandstone was collected from the bottom of another water well (250135 8792523) beneath a weathered layer of 11 to 12 meter thickness in the southern part of 1030SE.

Conglomerate

No outcrops of conglomerate were observed in the basal part of the Luitikila Formation despite the prediction that there would be some outcrops near the boundary between granitoids of basement complex and this formation. However, well-rounded pebble-sized floats of quartzite were found in several areas near the boundary. The floats also occur in a flat plain far from the river. This indicates that the floats would be in-situ products of weathered conglomerate, not fluvial deposits.

The pebbles excavated from another rwater well (N092203: 273141 8831852) comprise mainly pebbles of quartzite of 0.5 to 1 cm in diameter and minor pebbles of mica schist.

-1130NE Sheet

Medium- to fine-grained sandstone

Exposed sandstones are frequently found in the Lubaleshi River and occasionally in the Lulingila River. Outcrops of medium-grained reddish sandstone (FC090420: 268,236 8,739,782) occur in the Lubaleshi River. It is well sorted and sub-rounded. Bedding is 45°strike and 10°NW dip.

Reddish gray fine sandstone with cross lamination (A090202: 270941 8741896) interlays thin bands of a hematite-rich layer.

-1130SE Sheet

Fine sandstone

Fresh fine sandstone is generally dark gray in color, but most sandstone has been turned yellowish white to brown by weathering. The fine sandstone is hard with clear bedding and is well sorted. It is composed of rounded quartz, minor plagioclase and potash feldspar, and occasionally tiny spots of hematite of 0.2mm in diameter.

Grayish sandstone with clear bedding showing a 65°strike and 19°N dip (FC080705: 281,014 8,701,615) is exposed in the Kanchibia River (Fig. 5.2.3.1-14).

Fig. 5.2.3.1-14 Grayish sandstone (FC080705)

Micaceous sandstone with bedding showing a 113° strike and 19°N dip (FC081315: 273,299 8,698,910) is exposed in the Kanchibia River. White sandstone has been identified in the Luangoshi River (FC20080803: 267,348 8,691,312. Medium-grained sandstone with argillic feldspar collected from a water well (APD080801: 250,059 8,696,293）is yellowish brown in color due to weathering. The grayish fine sandstone (N072301: 276,724 8,700,207） is massive with no clear bedding.

Calcareous sandstone

Calcareous fine-grained sandstone occurs in some locations. The dark grayish calcareous sandstone has fine clastics of 0.1 to 0.2 mm in diameter and hematite spots.

Siltstone

The fresh siltstone is light gray to dark purple in color, but most siltstone has become yellowish white to brown yellow by weathering. The siltstone is soft, is often interlaid with a thin muddy layer of up to 5 mm in thickness. The siltstones occurring in the Luitikila River generally contain fine muscovite (φ0.1～0.2mm. The cleavage of siltstone is rich in muscovite.

An excellent outcrop of purplish gray siltstone 50 meters wide (N081306: 263,189 8,696,408) shows a 52° strike and 10°NW dip of bedding (Fig.5.2.3.1-15). This siltstone with minor muscovite is soft, and is interlaid by a thin muddy layer.

Fig.5.2.3.1-15 Left: Large-scale outcrop of purple to grey siltstone (N081306).
Right: Weathered micaceous siltstone with a muddy layer (N081203)

Siliceous schist containing minor calcite, muscovite and magnetite (FC20080702: 269,066 8,682,437) shows clear schistosity with a 63°strike and 10°SE dip

(4) Alluvium

Alluvium sediments cover a broad area of the western part of the 1130NE and 1130SE sheets. Narrow and thin alluvium deposits have also developed along small streams in all survey areas. Alluvium sediments consist mainly of fine- to medium-grained quartzose sands.

-1030NE sheet

Alluvium sediments cover a broad area of the Luombe River in the northeastern and downstream parts of the Lukulu River. Narrow and thin alluvium deposits have also developed along the small streams in the metasediments area. On the other hand, broad alluvium deposits have developed on the gentle slopes of the granitoids area. Alluvium sediments consist mainly of fine- to medium-grained quartzose sands (φ0.1～0.2ｍｍ) with minor feldspar and mica.

-1030SE sheet

Alluvium sediments cover a broad area along the Lubansenshi River and Chambeshi River. Narrow and thin alluvium deposits have also developed along small streams throughout thel survey area. The downstream areas of the Lukutu River and Muninshi River become broad alluvium deposits. Moreover, alluvium deposits are developing in a basin of 2 to 3km in diameter in the northeastern part. Alluvium sediments consist mainly of fine- to medium-grained rounded quartzose sands.

-1130NE sheet

Alluvium sediments cover a broad flat plain of the southwestern part of 1130NE. Narrow and thin

alluvium deposits have also developed along small streams throughout the survey area. A natural levee has developed along the Chambeshi River. Alluvium sediments consist mainly of fine- to medium-grained quartzose sands.

Pitting excavation for observation of alluvium was done in the Kabinga area (244,813 8,734,562)in the southwestern part of this study area. Sands from the pit consist mainly of fine- to medium-grained, rounded, poorly sorted quartzose sands. No sedimentary structure was observed in the pit wall due to bioturbution. Water level was under 190 cm.

Lake sediments are recognized in principal lakes such as Chaya Lake and Bemba Lake. The swamp zones near the lakes contain a black muddy layer that is rich in organic material.

-1130SE sheet

Alluvium sediments cover a broad area of the northwestern part of the 1130SE sheet. Narrow and thin alluvium deposits have also developed along small streams throughout the survey area. Alluvium sediments consist mainly of fine- to medium-grained quartzose sands with minor feldspars. Lake sediments occur in Bakabaka Lake. Poorly sorted sand and silt layers underlie a black muddy layer of 50 cm in depth.

5) Intrusive

(a) Metavolcanic

Dark greenish gray metavolcanic rock occurs in the upper reaches of the Mukanga River in the southwest part of the 1030NE sheet. It is massive, hard, coarse-grained and porphyritic, and lacks any evidence of flow banding. Quartz makes up the largest proportion of the rock. The metavolcanics contain minor pyrite and chalcopyrite of up to 3mm in diameter. The metavolcanics are silicious but no significant alterations are recognized. In some places, metavolcanics include concentrates of tuffaceous or fine-grained angular lithic fragments.

The metavolcanics seem to form a narrow belt with an E - W trend though their exposure is very limited. They seem to be uncomformably overlain by sedimentary rocks of the Mporokoso Group though no contact with other rock units was observed due to this poor exposure.

(b) Gabbro and Dolerite

Several outcrops of mafic dykes extending WNW-ESE occur mainly in the eastern part of 1030NE. These dark green to gray colored dykes are composed of pyroxene, olivine and feldspars. The pyroxene and olivine were transformed into chlorite or epidote by weak alteration. Weathered feldspar is up to 2 to 3mm, but is often micro crystals of less than 1mm. Dissemination of fine pyrite of 1mm or less in diameter can often be found in dykes.

Dark green medium-grained gabbro of 20m in width and >50m in length is exposed on the banks of the Samba-Lubemba River (Lh7100210: 258,638 8,885,853). It intrudes into the psammitic gneiss of the basement complex and occurs as small dykes that form a discontinuous exposure with a southwest trend. There is a chilled margin along the boundary of about 2m in width. Plagioclases in this dyke are generally 1 to 3 mm, with some fine crystals of less than 1mm. In rare instances, there are fine chalcopyrite crystals of less than 1mm.

In FC092228 (276,977 8,872,321) of the Lukulu River, there is a vein of intrusive rock with an E-W orientation that runs perpendicular to the stream.

(c) Microgranite

Outcrops of dark gray microgranite (Ld008: 278463 8879300)occur near the bridge on the road to Mporokoso. Microgranite is hard and massive. Fine phenocrysts of 0.1 to 0.5mm of quartz, potash feldspar, plagioclase, microcline, and muscovite have been observed

6) Hydrothermal veins

(a) Quartz veins

-1030NE

Irregular massive or lens types of quartz veinlets (Lh7100208: 258874 8888474)occur in metasediments of the basement complex. Pyrite, chalcopyrite, bornite, and pyrrhotite occur in quartz crystals or host rock near the veinlets. Coarse-grained crystals of chalcopyrite of up to 5mm are occasionally observed. The average homogenized temperature of fluid inclusions in irregular lens quartz veins is a relatively low 160°C and salinity is 7.5％NaCl eq.

Grayish chalcedonic quartz veins containing pyrite in a 20° strike occur in metasediments. Gold content in quartz veins is 0.003ppm, and silver is 0.28ppm.

Quartz veins accompanying specularite (M50: 257294 8862906) occur in the Mporokoso Formation. The veins show an E-W trend strike and 0.05ppm silver (Ag). Gold (Au) was under the detection limit.

A ridge-forming quartz vein extending toward 332° direction (N091503: 261,033 8,885,486) is exposed in metasediments. The quartz vein is massive and brecciated, and includes a boxwork of relict sulfides. Gold content in the quartz vein is under the detection limit, and silver is 0.09ppm.

A network of quartz veins (N091504: 262,155 8,886,464) has been observed in the Kasama Formation. The dominant trend of veinlets cutting quartzite is N-S. Gold content in the quartz veins is under the detection limit, and silver is 0.09ppm.

A network of quartz veins (A091702: 236,393 8,863,015) has also been observed in the Mporokoso Formation. Ridge-forming quartz veinlets extend approximately 2 km along a 285° strike. Gold

content in the quartz veins is under the detection limit, and silver is 0.12ppm.

-1030SE

White quartz veins (Lh7101601: 269047 8831124) occur in about 5m×20m size extending toward a 290° strike in the forest near the Munwa River. Joints or fractures have WNW or N-S trends. No ore mineral has been observed. Gold content in quartz veins is 0.001ppm.

Several quartz veins showing E-W trends of the dominant strike occur in the Lubansenshi River in the northwestern part.

-1130NE

Outcrops of sandstone with light grayish quartz veinlets (FC090422: 267384 8739422)occur in streams. The strike of quartz veins is 20°. Veins are narrow, only a few centimeters wide.

-1130SE

White to transparent quartz veins with black specularite has been observed. Vein outcrops are small in size: 16cm in width and 3m in length. Gold content in quartz veins is under the detection limit. Many floats of quartz veins occur near the outcrops. Local people crush these quartz floats to make industrial materials.

(b) Pegmatite

Pegmatites of coarse crystals composed of muscovite, quartz, tourmaline and feldspar occur in granitoids and metasediments. Pegmatite forms dyke shape in maximum 2 to 5 mm width. Large crystals of quartz and muscovite over 5 cm is observed in representative outcrop (LI7100301: 259,521 8,879,529） in Lukulu River.

Lens or dyke shaped pegmatite composed of course feldspar and muscovite occurs parallel to banded structure of metasediments in northwestern part (Lh7091103: 227694 8889227). Ruins of excavated pits for pegmatite often exist around this area.

Fig. 5.2.3.1-16　Lens-shaped pegmatite in metasediments (Lh7091103)

7) Weathered layer, colluvium

A weathered layer or colluvium, which covers the surface of the entire survey area, is strongly weathered or reworked material of the basement complex, the Muva Supergroup and the Katanga Group. This layer comprises lateritic sand or clayey soil which is utilized for house and road construction. Maczka and Cap's (1973) survey of surface deposits by hand auger in the Lukulu River in 1030NE found dark gray to grayish sandy and silty clay from surface to 2m depth, and clay containing weathered pebbles of mica schist from 2m depth to 3m depth.

Laterite-rich pebbles have been observed from the surface to 2-3m depth in a quarry (N091303:266166 8862916)in Mporokoso Formation. Sub-rounded cobbles of quartzite are dominant from that depth. Quartzite and shale are exposed at the bottom of quarry.

Ruins of small-scale mining operations for iron-rich laterite exist near old iron smelting kilns (263277 8852161）.

-1030SE Sheet

According to the information on water wells in local villages, the weathered horizon (B horizon) is about 7 – 15m thick around the Luitikila Formation. Weathered sandstone (C horizon) with strongly weathered feldspar underlies the B horizon.

-1130SE Sheet

Pit excavation in Chalabesa Village (283166 8,741,614) was made to research the soil profile. Survey results are as follows

0～0.3m: Light brown organic rich sand (A-horizon)

0.3～0.8m:Yellowish light brown medium- to coarse-grained sand

0.8～2.4m: Reddish brown to orange sand with plant roots

2.4～2.6m(Bottom of pit): Angular gravel pebbles and cobbles of quartzite, sandstone, and

siltstone.

-1130SE Sheet

Pit excavation in Kopa Village (263,474 8,696,880) was made to research the soil profile. Survey results are as follows:

0～0.1m: Organic rich black layer(A-horizon)

0.1～1.0m: Bioturbated fine sand with plants roots

1.0～1.7m: Fine sand with minor gravels

1.7～2.85m: Pebbles of siltstone, sandstone and quartz veins are dominant. Pebbles are sub-rounded to sub-angular, with an average size of φ10mm.

2.85～3.3m(Bottom of pit)：Highly weathered clayey siltstone.

In Njeke village (280,359 8,712,560), neither base rocks nor pebbles could be exposed by excavation until 3.7m in depth.

0～0.2m：Organic rich black layer (A-horizon)

0.2～2.8m：Reddish brown sandy soil

2.8～3.6m：Brownish sandy soil

3.6～3.7m(bottom of pit)：Very soft, strongly weathered light gray clayey sandstone.

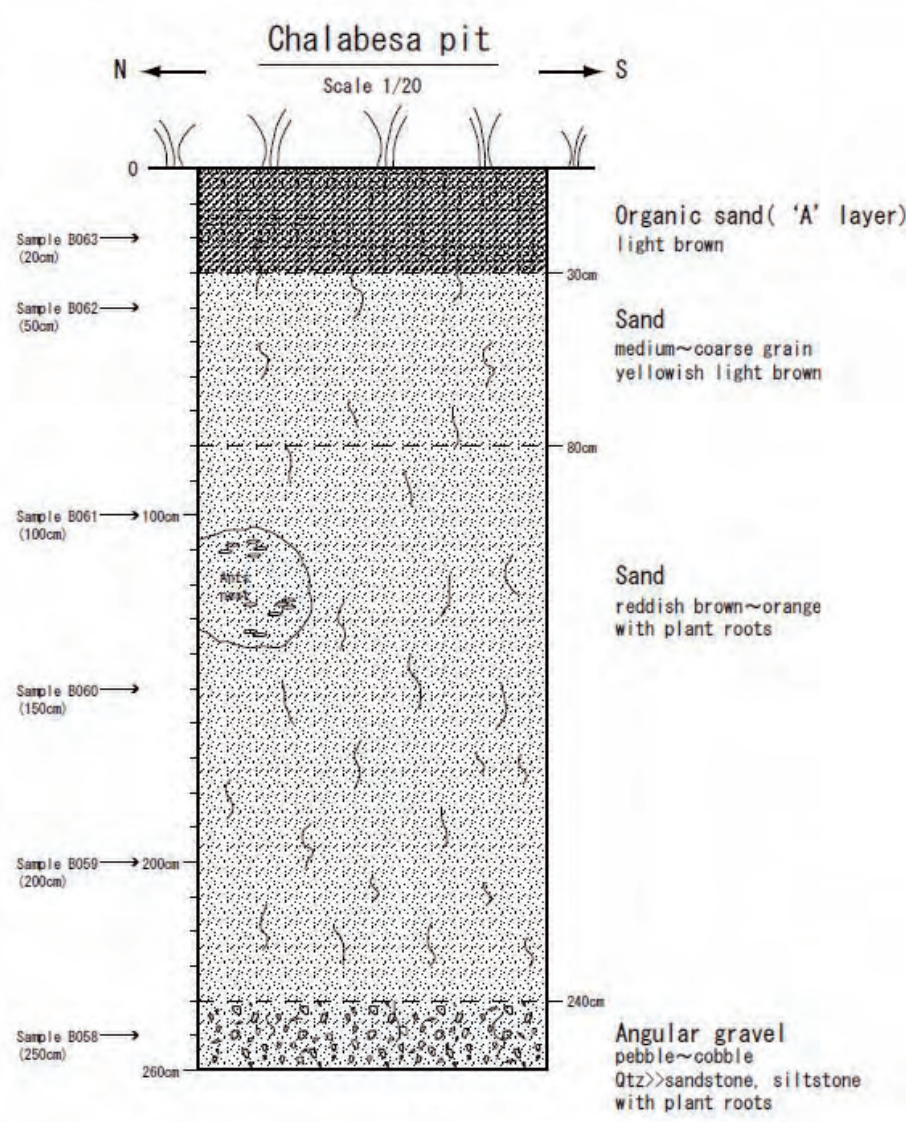

図 5.2.3.1-17 Observation of Chalabesa Pit

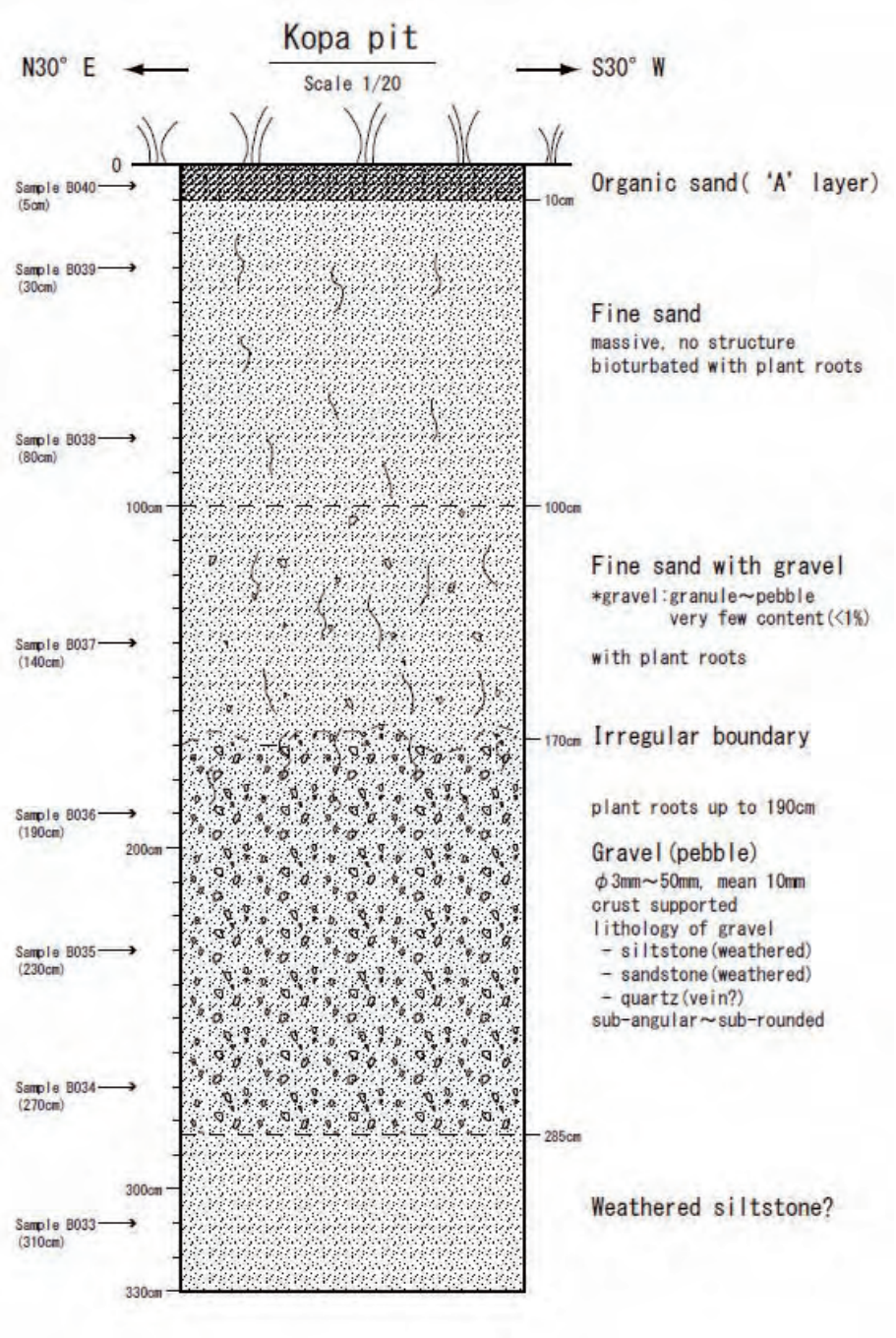

図 5.2.3.1-18 Observation of Kopa Pit

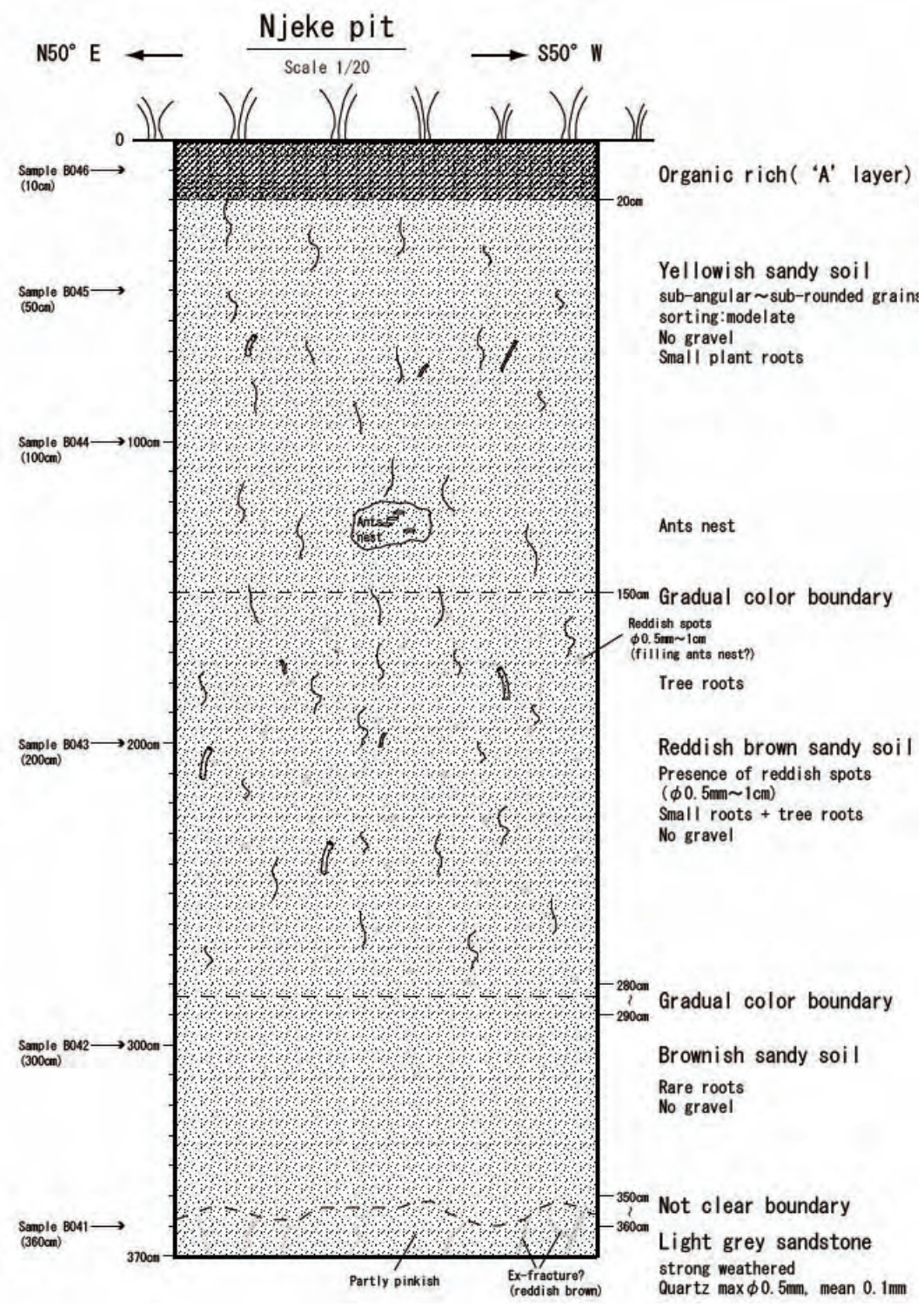

図 5.2.3.1-19 Observation of Njeke Pit

5.2.3.2 Geological Structure

The dominant geological structure is deduced from geomorphological features in multi-shading images from SRTM/DEM.

(1) 1030NE map sheet area

Varieties of foliations (schistosity, gneissic structure) are well-developed in the granitic gneiss and metasediment of the basement complex. The foliations generally show strikes ranging from N60W to N80W in direction. A rose diagram of these foliations that were observed in the basement complex (Fig. 5.2.3.2-1) shows distinct WNW-ESE directional concentration.

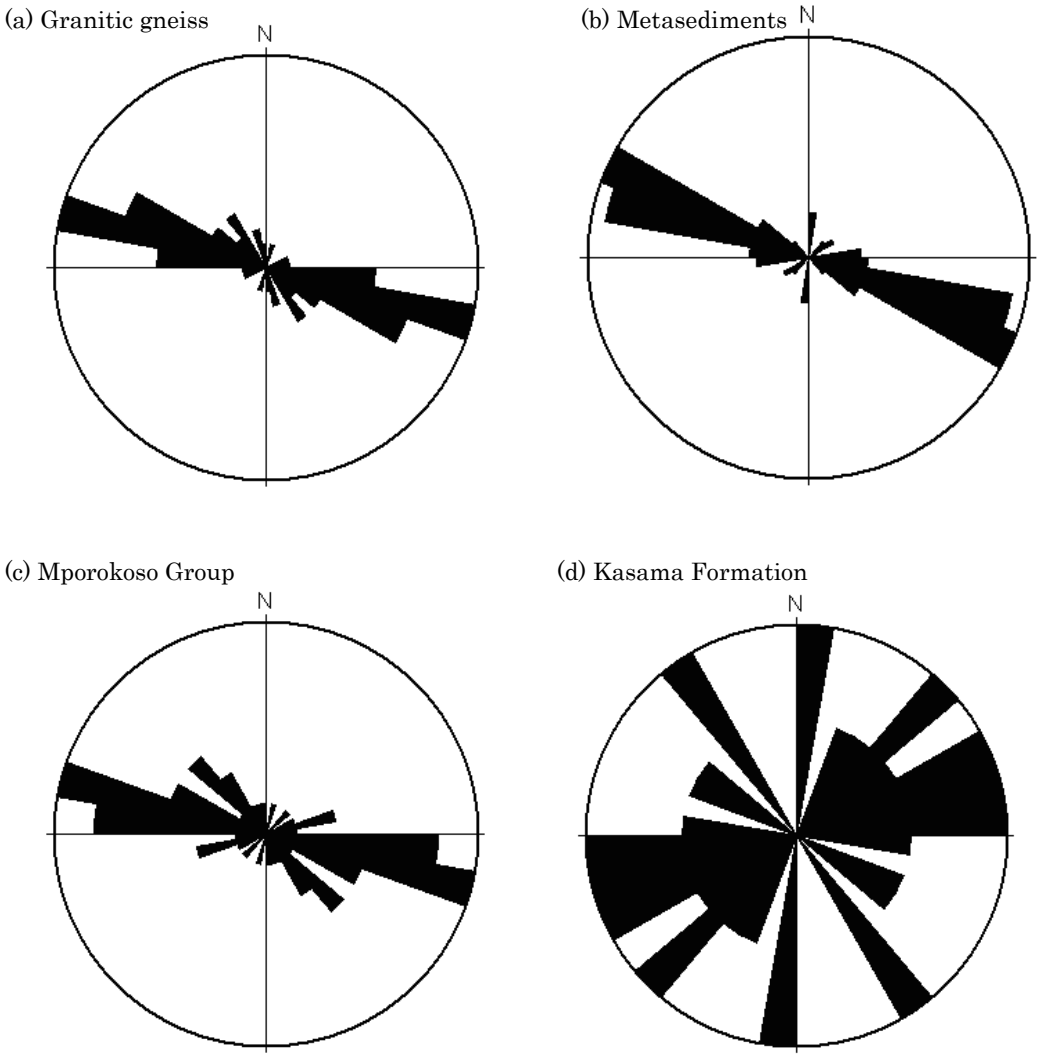

Fig. 5.2.3.2-1 Rose Diagram of Bedding and Foliation Directions (1030NE sheet area)

The quartzite sequence of the Mporokoso Group comprises an isolated hill range in the central part of the area. It shows north and south dipping into a basin syncline which has E-W to ESE-WNW strikes. The quartzite sequence of the Kasama Formation comprises an isolated hill range in the northeastern part of the area. Its bedding plains show various directions but the strike tends to range from the NE-SW to E-W directions. This suggests that the Kasama Formation has a N-S oriented synclinal structure. The Luombe River runs along the syncline axis.

The multi-shading image in Fig.5.2.3.2-2 shows a distinct topographic feature related to the geological structure of the bedrock. A smooth topographical texture is generally depicted in multi-shading images because stream systems develop poorly in a hard and compact rock sequence like quartzite. Smooth textured domains have developed in the central and northeastern parts of the sheet area which coincide with distributions of quartzite of the Mporokoso Group and Kasama Formation, respectively. This demonstrates the powerful expressiveness of multi-shading images.

Stream systems are rather well-developed except in domains of quartzite. They show topographic features of a basement complex (granitic rock, metasediment). Continuous white and black contrasted rims run along the boundary between the basement complex and the quartzite of Mporokoso Group and Kasama Formation. They are assumed to be cliffs or ridges where quartzite outcrops are exposed.

Series of WNW-ESE or N-S oriented lineaments and faults can be clearly seen in Fig 5.2.3.2-2, especially a straight WNW-ESE oriented fault which can be distinctly traced in the southwestern margin of the Kasama Formation. A parallelistic lineament also has developed in the Luluku River 10km south of it. Mica schist and pelitic schist are distributed along the Luluku River. Their schistosity is predominant in the WNW-ESE direction. These findings suggest that the lineament reflects the direction of the schistosity.

A WNW-ENE oriented shear zone was discovered during the geological field survey in the quartzite of the Mporokoso Group and Kasama Formation. A number of fractures have developed parallel to the shear zone although fractures are generally poor in other substantial outcrops of the quartzite. N-S oriented shear zones have also been observed in the Mporokoso Group and Kasama Formation.

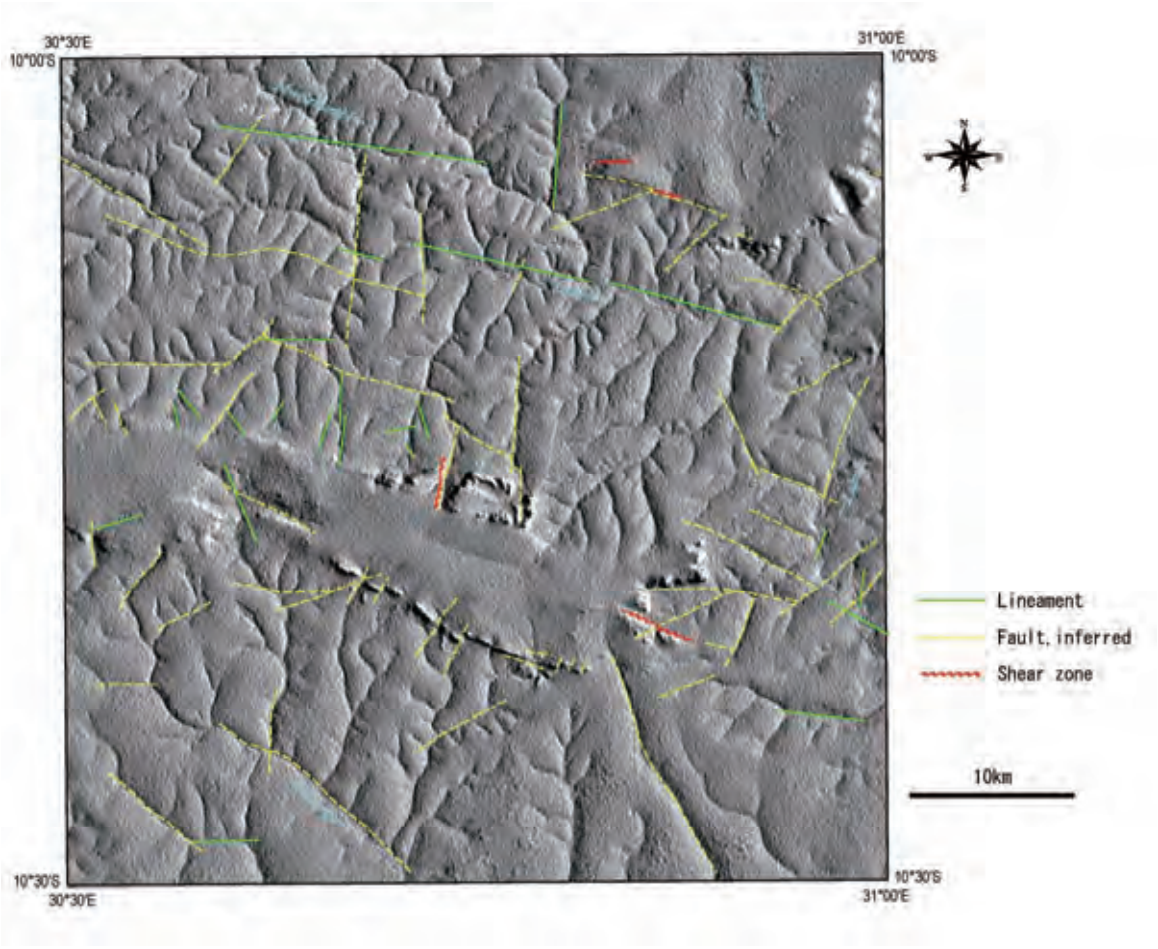

Fig. 5.2.3.2-2. Multi-shading Image Generated from SRTM DEM (1030NE sheet area)

(2) 1030SE map sheet area

The 1030SE sheet area has a low relief profile. The development of drainage systems is inferior to the 1030NE sheet area. The sheet has been divided into the following two domains based on the topographic features shown in the multi-shading image (Fig. 5.2.3.2-3) and observations made during the geologic field survey:

a) The northern margin zone characterized by somewhat distinct drainage development, and b) the rest of this sheet (all other areas).

The northern zone corresponds to the distribution of granitic rocks (Gr) of the basement complex. Drainage patterns oriented from north to south have developed there. However, typical geological structures have not been distinguished.

Area b) corresponds to the Luitikila Formation, and geological features are not discernable due to the lack of undulation. However, the boundary between areas a) and b) suggests a geological boundary with an E-W orientation, represented by the green arrows in the image below.

In the central to eastern spreading part of Area b), there is a slight undulation which is more recognizable compared with the western part. Moreover, basin structures of 2 to 3km in diameter have developed in the northeastern part. Their geographical features might have been formed by the marshy ground called “dambo” which is common in this area. These marshy basins resemble “doline” landforms that often develop in limestone areas. Calcareous sandstone is presumed to occur in this part, although its outcrops have not been observed.

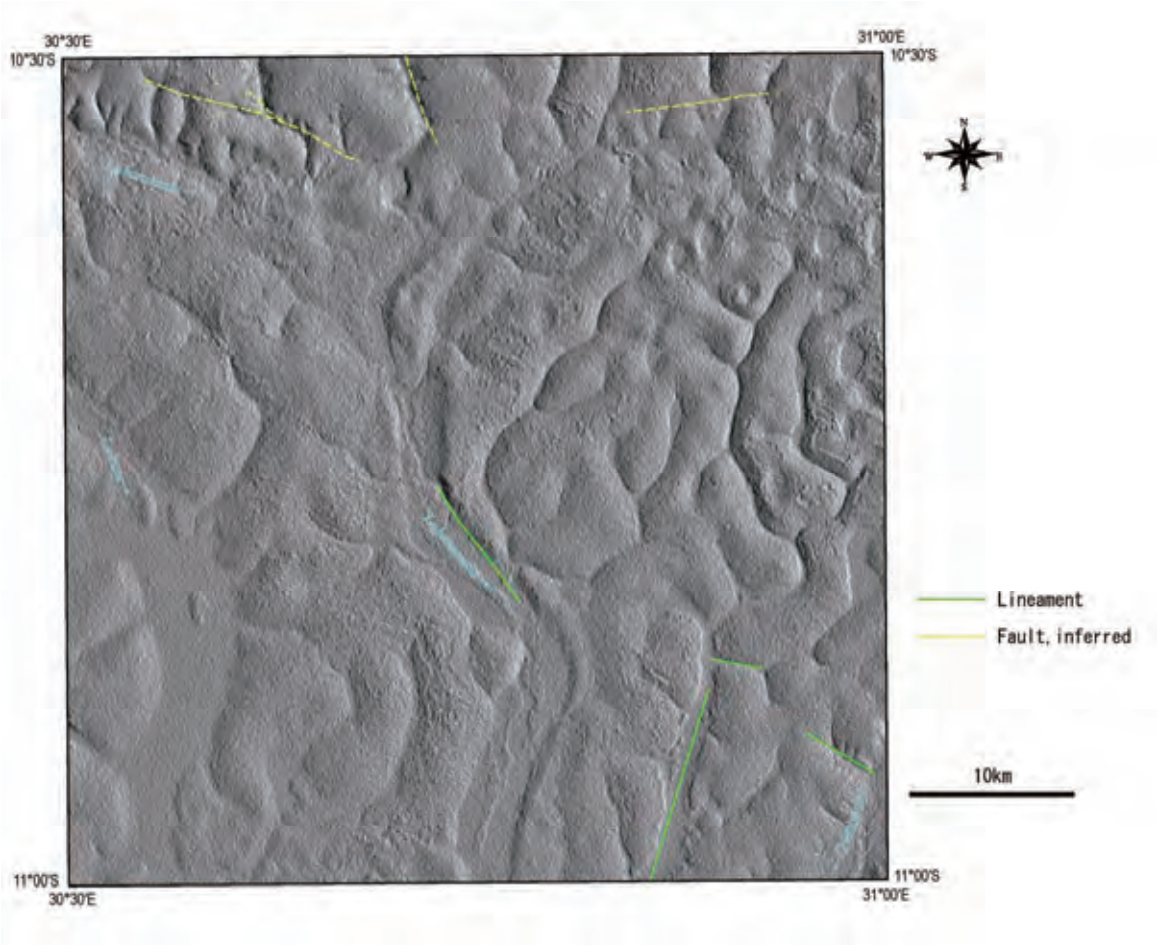

Fig. 5.2.3.2-3. Multi-shading Image Generated from SRTM DEM (1030SE sheet area)

(3) 1130NE map sheet area

The 1130NE sheet area is characterized by a low relief profile and a flat plain. Three topographic domains are delineated by multi-shading images made from SRTM/DEM (Fig. 5.2.3.2-4) as follows: a) the eastern part characterized by short and straight streams, b) the northwestern part characterized by jaggy relief and meandering marsh (dambo) and c) the flat plain of the southwestern part.

NE-SW and NW-SE oriented streams are well-developed in the southwestern part. Strikes of sandstone beds observed during detailed geologic surveys are predominant in the NE-SE direction

(Fig. 5.2.3.2-5). The sandstone beds incline gently up to 30°. Dipping of 0° to 10° toward the northwest is common.

Dambos (the local term for marshes or small depressions) are well-developed in the northwestern part. The occurrence of Calcareous sandstone is presumed by the doline-like dambos, although its outcrops have not been reported. A NNE-SSW oriented fault is inferred to be the boundary between the northwestern part and the eastern part located along the Chambeshi River by its topographic contrast.

The flat plain of the southwestern part is an alluvial plain formed by the Chambeshi River. Natural microtopographic levees have formed along the river channel.

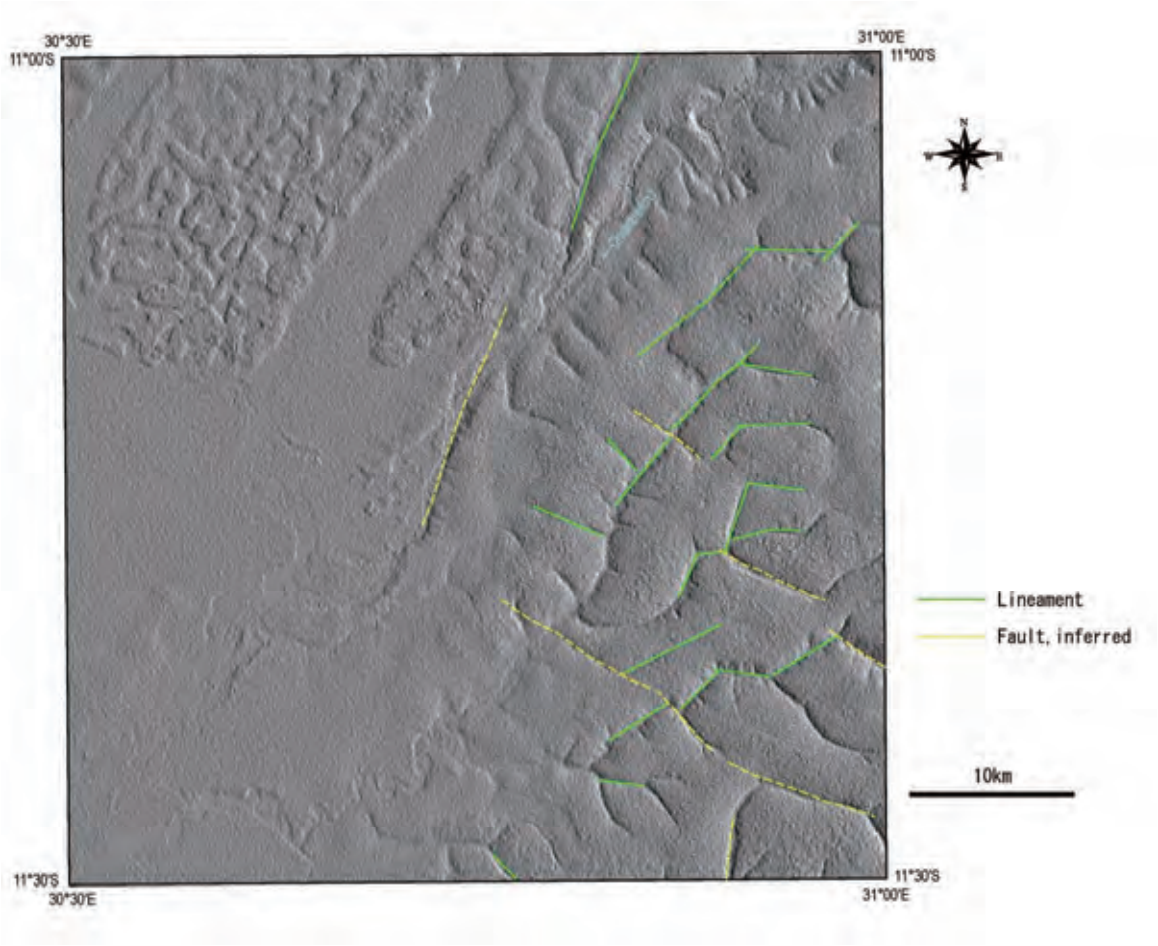

Fig. 5.2.3.2-4 Multi-shading Image Generated from SRTM DEM (1130NE sheet area)

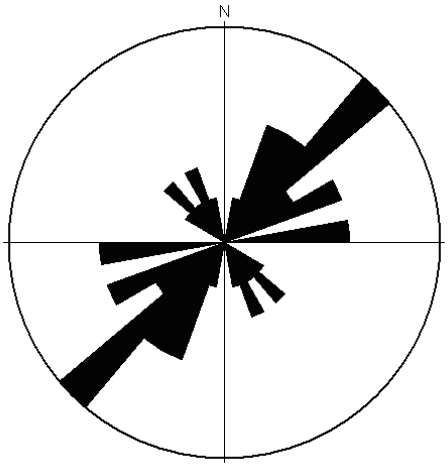

Fig. 5.2.3.2-5 Rose Diagram of Bedding Directions (1130NE sheet area)

(4) 1130SE map sheet area

Dissection topography, which is characterized by a number of short streams flowing into the Kanchibia River and Luitikila River, is well-developed, in addition to the NE-SW and NW-SE oriented short and straight streams mentioned above (Fig 5.2.3.2-6). The two rivers provide the main drainage of this sheet area. Bedrock along the two rivers is relatively well exposed, because downward erosion by the two rivers is deeper, while outcrops are rarely found along the other, smaller rivers. Strikes of the Luitikila Formation are mainly oriented in the NE-SW direction as shown in the rose diagram (Fig. 5.2.3.2-7). The dips are up to 30°, and are mainly 10° to 20° NW.

NW-SE oriented lineaments are predominant in the northern part of the sheet area.

In the northwestern part of the sheet area, a flat alluvial plain covers much of the surface.

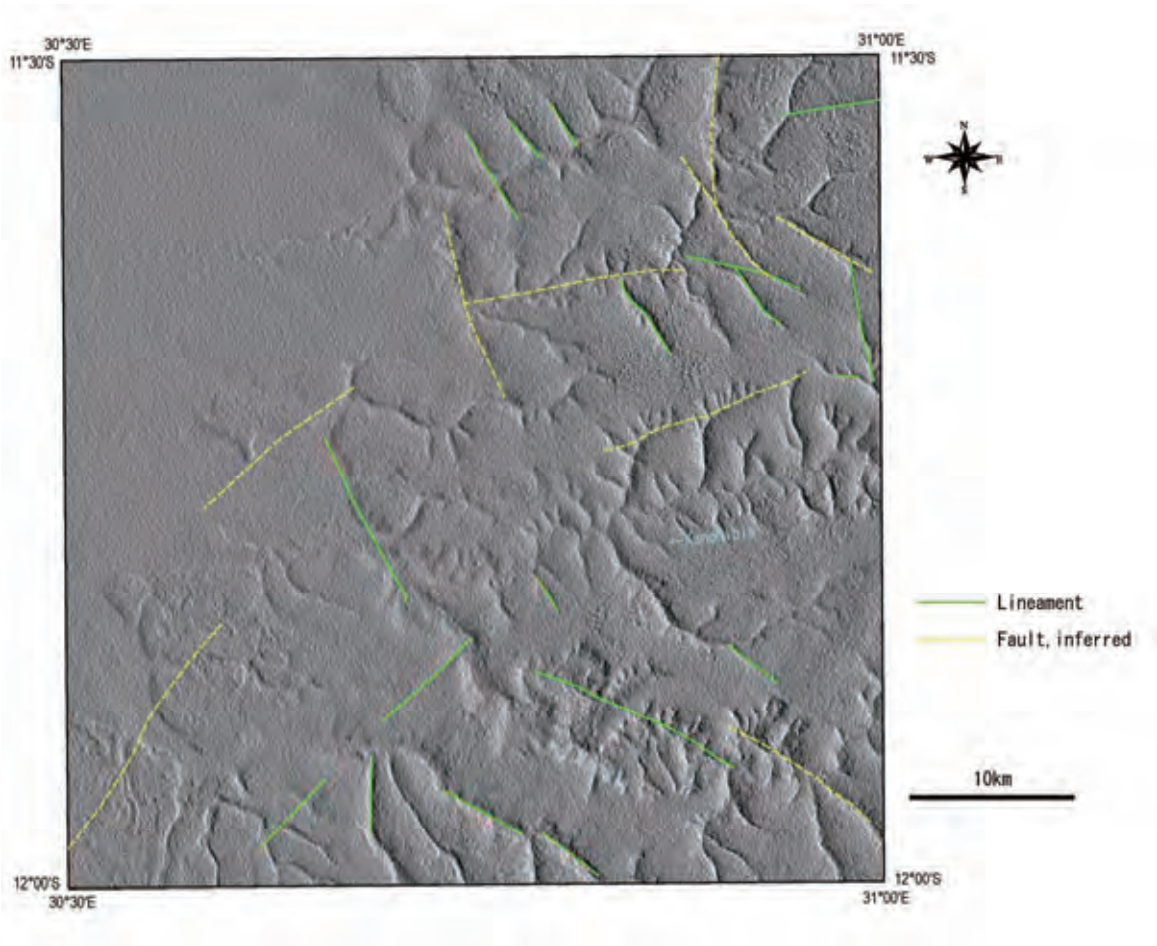

Fig. 5.2.3.2-6 Multi-shading Image Generated from SRTM DEM (1130SE sheet area)

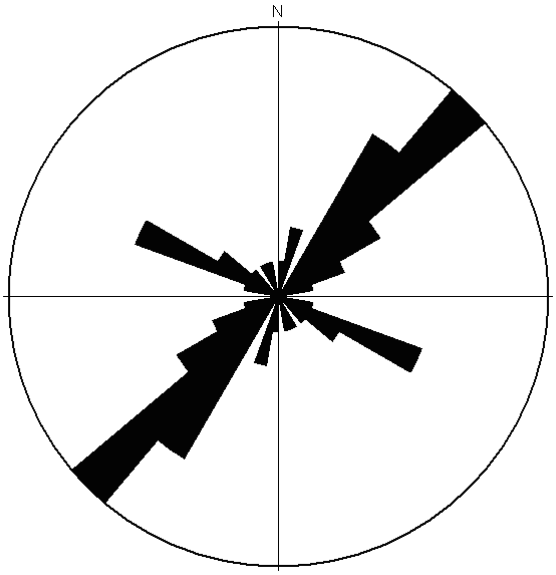

Fig. 5.2.3.2-7 Rose Diagram of Bedding Directions (1130SE sheet area)

5.2.3.3 Mineralizaion

(1) Copper

Three very weak mineral occurrences of copper have been confirmed in the 1030NE sheet area (Table 5.2.3.3-1). Locations of mineral occurrences, and the results of microscopic observation and chemical analysis are shown in Fig. 5.2.3.3-1, Appendix V-9, and Appendix V-10, respectively. The occurrences are named Mukanga, Samba Lubemba South and Samba Lubemba from the west to the north, and are described below.

Table 5.2.3.3-1 Mineral Occurrences in the Survey area

Location No.	Polish section No.	Coordinate(ARC1950)		Stream Name	Mineral Assemblage	Host/Contact Rock	Formation
		N	E				
Lh7090721	Ph-03	8,863,933	237,074	Mukanga	Cp	Metavolcanic	Basement Complex
Lh7100208	Ph-01	8,888,474	258,874	Samba-Lubemba	Cp>Py-Po	Quartz vein	Vein
Lh7100210	Ph-02	8,885,853	258,638	Samba-Lubemba South	Py>>Cp	Gabbro	Dyke

Cp: Chalcopyrite, Po:Pyrrhotite, Py: Pyrite

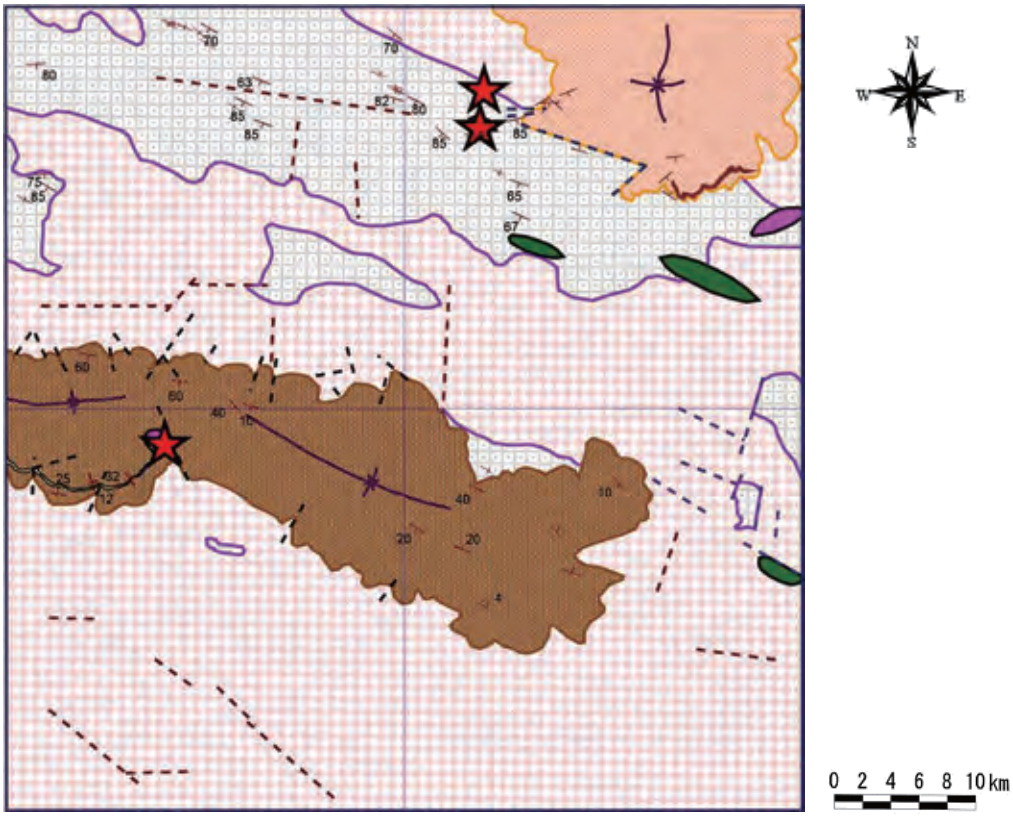

Fig. 5.2.3.3-1 Locations of Mineral Occurrences

(1) Mukanga Occurrence

Chalcopyrite occurs in bluish grey or light green colored metavolcanics. Metavolcanics of 1km in

length (E-W) and 400m in width (N-S) crop out in the upper reaches of the Mukanga River. The chalcopyrite occurs as idiomorphic or hypidiomorphic small grains, with maximum size being a few millimeters. A few grains of chalcopyrite are scattered per square meter. These grains disseminate in the matrix of the metavolcanics. The metavolcanics are weakly silicified but no significant alterations are recognized. In some places, metavolcanics include concentrates of tuffaceous or fine-grained angular lithic fragments (Fig. 5.2.3.3-2 left).

Chemical analysis of metavolcanics showed low values, 22ppm Cu and 0.02% S, indicating no economic significance of Cu.

Fig. 5.2.3.3-2 Metavolcanic rock in the Mukanga Mineral Occurrence (left), and Quartz Vein in metasediments in the Samba Lubemba Mineral Occurrence (right)

(2) Samba Lubemba South Occurrence

Pyrite is disseminated in gabbroic rocks around the boundary with the psammitic schist. A gabbroic dyke intrudes the psammitic schist of the basement complex. It is exposed in a 100m X 20m area with a WNW-ESE trend along the Samba Lubemba River. No significant argilic alterations were detected in the gabbroic dyke. A 2m wide child margin has developed in the gabbroic dyke at the contact point with psammitic gneiss. The psammitic gneiss near the contact shows drag deformation caused by the dyke intrusion.

Chemical analysis of this dyke showed 51ppm Cu and 0.08% S. The copper content is consistent with the background level of basic dykes.

(3) Samba Lubemba Occurrence

Chalcopyrite and pyrite mineral occurrences were observed in quartz veins hosted by migmatitic metasediments on the banks of the Samba-Lubemba River. Granite or pegmatite dykes irregularly penetrate into the basement psammitic gneiss at this outcrop. Chalcopyrites, bornites and pyrites occur in the quartz veins (Lh7100208) which are parallel to the foliation at the contact point between

the granite and the psammitic schist (Fig.5.2.3.3-2, right). It appears that the mineralization is related to the granite activity, although a segregation origin could also be inferred from the irregular shape of the quartz veins.

Copper and sulfur anomaly values of 151ppm Cu and 1.36% S were detected by chemical analysis of this quartz vein. The small scale of the quartz veins and their low Cu content indicate no economic significance.

(4) Gold

A number of quartz veins occur in the survey area. The quartz veins are a few centimeters to a few meters in width and occasionally extend a few kilometers in length. No ore minerals have been observed in the quartz veins. A network zone of NW-SE trending quartz veins has developed in the lower reaches of the Mukanga River. The zone is a maximum 3 meters in width and forms ridge topography (Fig. 5.2.3.3-3). Several quartz veins analyzed by this study have no anomaly value. Most of the Au values are under the detection limit.

In the 1980's, exploration work targeting placer gold deposits was conducted in basal conglomerate of the Mporokoso Group in the Mbala-Kasama area located in the northern part of the survey area. Andrews-Speed（1982）reported Au concentrations of up to 0.35ppm by channel sampling focused conglomerate. He concluded that the basal conglomerate had high potential for placer gold deposits. The basal conglomerate layer of the Mporokoso formation observed in this sheet was very thin, estimated to be less than 10m thick. There are few outcrops in this sheet due to poor exposure. A one-meter size conglomerate float near the Futaba River (N091606;256353 8864370) has some gold, but under the detection limit.

Fig. 5.2.3.3-3 Quartz Ridge in the Lower Reaches of the Mukanga River (left)

(3) Laterite

The ruins of an old iron smelting kiln were found near the Kubundi River. Floats of iron slag were also observed in this sheet area. Low-grade laterite ridges with rounded to sub-rounded pebbles

filled by hematite and limonite were often observed. All laterite deposits are too small in scale to have any economic value.

5.2.3.4 Dating Analysis

EPMA dating analysis is carried out to estimate the forming age of each lithological formation. In the EPMA dating method, age is estimated by the volume ratio of U, Th and Pb contained in zircon or monazite in the sample rock (Appendix V-11). The dating analyses were conducted at the Japanese National Museum of Nature and Science in Tokyo.

Zircon and Monazite in igneous rock indicate its forming age. In the case of sedimentary rock, the EPMA ages of detrital zircon and monazite generally do not coincide with the sedimentary age of the formation, but rather indicate the age of the zircon or monazite grains which originally formed in the source rocks. Thus, EPMA dating may give information on possibly the maximum deposition age of sedimentary rock.

In general, EPMA dating of monazite is more accurate than zircon because monazite has higher Th content than zircon. But, monazite is vulnerable to metamorphism, so dating results may reflect the metamorphic age, not the formation age due to thermal resetting. Thus, careful interpretation of dating results is required.

(1) 1030NE sheet

The dating results of rocks sampled in the 1030 NE sheet area are shown in Table 5.2.3.4-1

Metasediments of the basement complex

The results of dating of psammitic gneiss from the Kapalu River (Dh-02) indicated a narrow range of monazite age of 2.03±0.03 to 1.92±0.02Ga and a wide range of zircon age of 2.33±0.20 to 1.87±0.12Ga. Error of dating (σ) in zircon dating is relatively large since U and Th content in zircon is less than monazite. Dating of monazite possibly reflects the metamorphic age because the psammitic gneiss is strongly deformed.

The results of dating of psammitic schist from the Mukoba River (RB020D) indicated a narrow range of monazite age of 2.02±0.02 to 1.92±0.01Ga and a wide range of zircon age of 2.90±0.14 to 2.16±0.24Ga showing bimodal picks around 2.85Ga and 2.35Ga. On the other hand, dating of monazite showed a narrow range of age at peak of 1.97Ga, though the age of detrital monazites generally vary greatly depending on their origin, as is the case with zircon. The difference between zircon and monazite dating is presumed to have been caused by the resetting of the formation age due to this metamorphosis.

The two strongly deformed metasediments samples in Mulungwizi gneiss belt described above have the same age of monazite from 1.94Ga to 2.00Ga. This monazite age suggests the rock was deformed during the Ubendian Orogeny (2.10-1.95Ga).

Granitoids of the basement complex

The dating of zircon in gneissose granite with weak foliation (RC012D) showed an average formation age of 2.22±0.17Ga. The dating of zircon in the gneissose granite part of migmatite (RB016D) showed an average formation age of 2.09±0.17Ga. No monazite was detected in either granite.

Dating results of metamorphic rocks suggested that granitoids were formed in the Pre-Ubendian period and were weakly deformed in 1.94- 2.00Ga.

Metavolcanics of the basement complex

The dating of zircon in metavolcanics in the Mukanga River (RA008D) showed an average formation age of 2.05±0.13Ga. Metavolcanics looked like younger rocks that had intruded into quartzite because the metavolcanics were surrounded by quartzite of the Mporokoso formation, though outcrops are not continuous. However, dating results revealed metavolcanics to be older than quartzite.

Muva Supergroup（Fig 5.2.3.4-2）

Four samples of quartzite from the Mporokoso Group were analyzed for EPMA dating. Only one sample included monazite for dating. Two monazite grains were measured by EPMA dating and the results showed an age of 20.4±0.2 Ga.

On the other hand, the zircon age of the Mporokoso Formation showed a wide range, from 3.63±0.31 to 1.8±0.17 Ga. This means that the Mporokoso Formation formed after 1.8 Ga. Daly and Unrug (1982) maintained that the Mporokoso formation was formed between 1.85Ga (after Eburnean Orogeny) and 1.10Ga (before Kibaran Orogeny). De Waele and Fitzsimons(2007) concluded that the Mporokoso formation was deposited after 1.82±0.02Ga by SHRIMP U-Pb dating methods of detrital zircon from the Mporokoso formation in the Mansa Region.

In the Kasama Formation, an age of 1.24±0.14 to 1.03±0.14 Ga was obtained from monazites and 3.16±0.39 to 1.74±0.14 Ga was obtained from zircons in two quartzite samples (No.6 and RB015D).

The detrital monazites of the Kasama Formation show very little thorium content. This may indicate evidence of thorium content resetting caused by some thermal event. Therefore, the monazite age (1.24±0.14 to 1.03±0.14 Ga) of the Kasama Formation may indicate some metamorphic event, whereas the zircon age of the Kasama Formation has a very wide range (3.19±0.39～1.74±0.14 Ga). Generally, the EPMA age of zircon is not affected by thermal history. Therefore it is assumed that the detrital zircon age indicates the forming ages of zircon derived from various sources, and suggests a maximum deposition age of 1.74±0.14 Ga. The monazite age indicates the secondary thermal resetting (metamorphism). Quartzites of the Kasama formation seem to have formed after the Ubendian Orgeny (2.1 – 1.95 Ga) and deformed during the Kibaran Orgeny (1.35 – 1.1 Ga).

A detailed lithostratigraphic study by Daly and Unrug (1982) suggested that the Kasama Formation was formed by the reworking of Mporokoso Group quartzites. An isotropic dating study by De Waele and Fitzsimons (2004) reported a zircon age of 1.43±0.01 Ga for the Kasama Formation, even though most of the samples indicated an age of approximately 1.9 Ga in the Formation. This suggests that the 1.43±0.01 Ga age indicates a reworking of the Mporokoso Formation into the new Kasama Formation, and the older 1.9 Ga age indicates primary deposition of the Mporokoso Formation.

Table 5.2.3.4-1 The Results of EPMA Dating Analysis (1)

Formation	Rock	Sample No.	Outcrop No.	UTM(N)	UTM(E)	Mineral	Age (100Ma)
Basement Complex (Mulungwizi Gneiss Group)	Psammitic Gneiss	Dh-02	Lh7062605	8,881,636	228,108	Monazite	20.3±0.3 ～ 19.2±0.2
						Zircon	23.3±2.0 ～ 18.7±1.2
	Psammitic Schist	RB020D	N091505	8,885,626	260,920	Monazite	20.2±0.2 ～ 19.2±0.1
						Zircon	29.0±1.4 ～ 21.6±2.4
Basement Complex (Granitoid)	Gneissose Granite	RC012D	FC091929	8,868,852	244,690	Zircon	25.6±2.9 ～ 19.6±2.4
	Gneissose Granite	RB016D	N091602	8,863,176	260,668	Zircon	24.3±3.8 ～ 18.0±2.8
Basement Complex (Intrusive)	Meta Volcanic	RA008D	Lh7090721	8,863,933	237,074	Zircon	24.3±2.0 ～ 18.6±1.8
Muva Supergroup (Mporokoso Group)	Quartzite	No.1	Lh7030301	8,856,188	263,075	Zircon	29.1±2.5 ～ 18.6±1.7
	Quartzite	No.2	Lh7030302	8,853,314	265,149	Monazite	20.4±0.1 ～ 20.4±0.2
						Zircon	36.3±3.1 ～ 18.7±2.1
	Quartzite	No.3-2	Lh7030303	8,855,924	263,197	Zircon	27.9±1.9 ～ 18.0±1.7
	Quartzite	No.4	Lh7030304	8,856,380	263,094	Zircon	27.5±2.4 ～ 18.6±1.8
Muva Supergroup (Kasama Formation)	Quartzite	No.6	Lh7030306	8,883,852	268,641	Monazite	12.4±1.4 ～ 10.3±1.4
						Zircon	30.4±4.0 ～ 17.4±1.4
	Quartzite	RB015D	N091505	8,886,747	262,593	Zircon	31.6±3.9 ～ 18.7±2.6

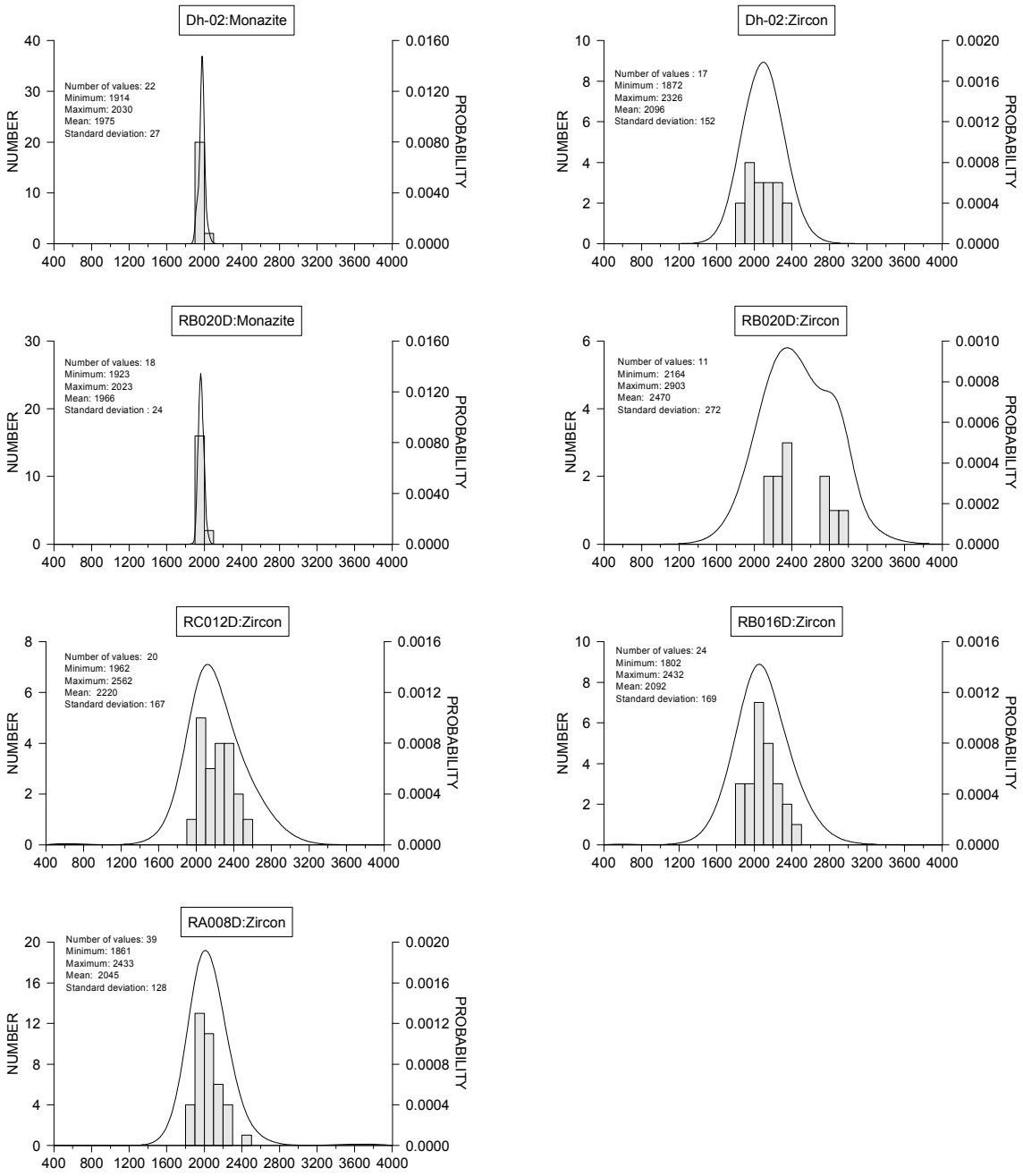

Fig 5.2.3.4-1 U-Th-Pb Monazite Ages and Zircon Ages of Basement Complex.

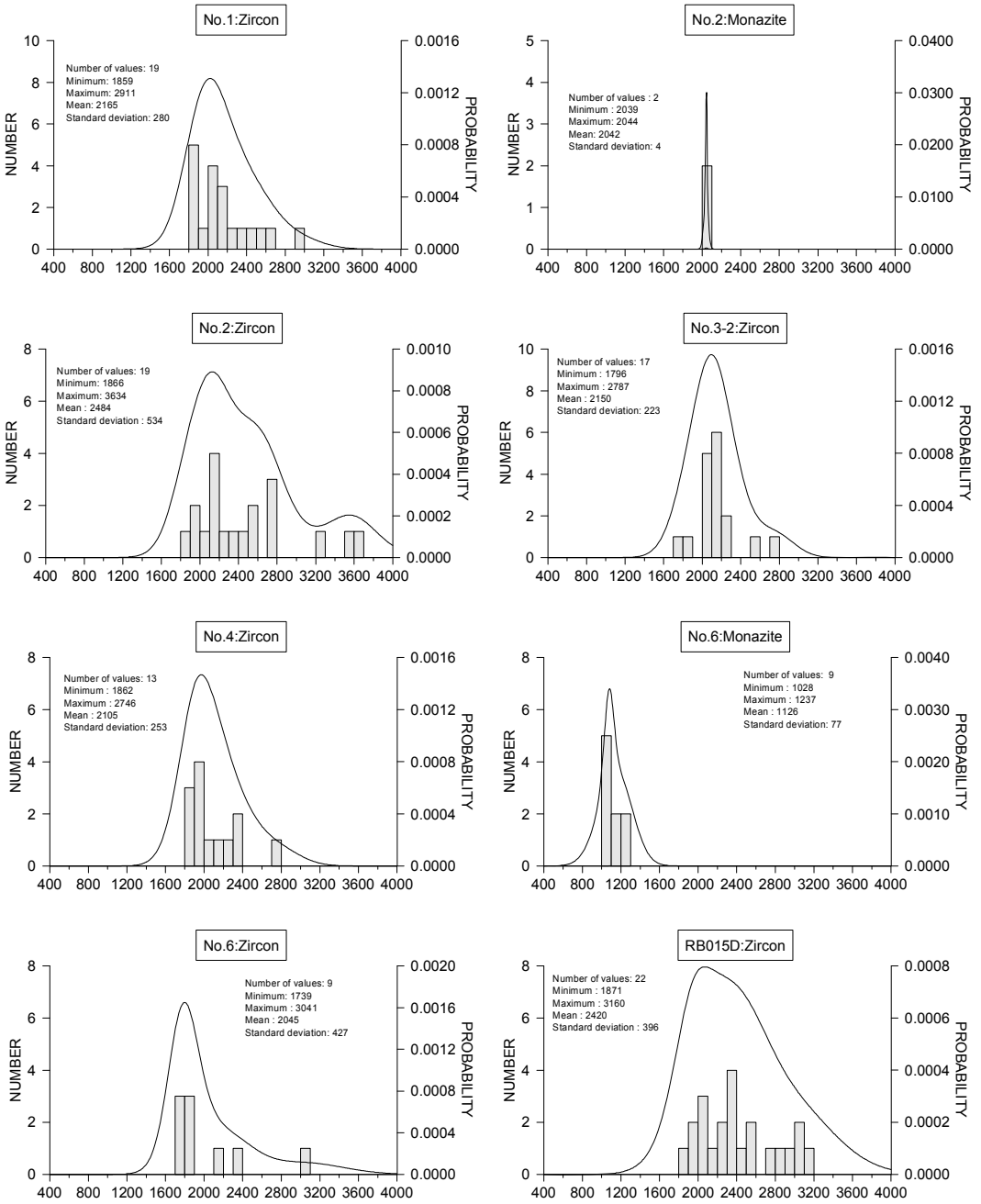

Fig 5.2.3.4-2 U-Th-Pb Detrital Monazite Ages and Detrital Zircon Ages of Muva Supergroup.

(2)1030SE Sheet

The dating results of rocks sampled in 1030 SE sheet area are shown Table 5.2.3.4-2 and Fig. 5.2.3.4-3.

Granite of the Basement complex

Dating results of monazites in granite (RA006) from the Lubansenshi River ranged from 2.00±0.02 to 1.75±0.05 Ga, averaging 1.93±0.04 Ga. The age of zircons shows a wide range since granite includes xenoliths. Xenocryst zircons have an older age ranging 2.94±0.21 to 2.50±0.15 Ga, while other zircon show a peak at approximately 2.1Ga.

Luitikila Formation

The age derived from the detrital monazite contained in red sandstone samples (Dh-01，Lh7103102) taken from the Chambeshi River ranged from 1.90±0.03 to 0.93±0.19 Ga with two peaks at 1.9Ga and 10.5Ga. The age of detrital zircon ranged from 2.48±0.33 to 0.65±0.03Ga with three peaks at 2.3Ga, 1.2Ga and 0.65Ga. The youngest age of 0.65±0.03Ga suggests that this formation was deposited after 0.65±0.03Ga.

In addition, the age obtained from the monazite contained in reddish sandstone (DI-01，LI07101501) taken from the Lubansenshi River shows a range of 1.04±0.18 to 0.63±0.03 Ga. The age derived from detrital zircon ranged from 2.15±0.27 to 0.76±0.03 Ga. The youngest age of 0.63±0.03Ga suggests that this formation was deposited after 0.63±0.03Ga.

In the vicinity of the study area, at least 3 orogenic events have occurred: the Ubendian Orogeny (2.1- 1.95 Ga), the Kibaran Orogeny (1.35-1.1 Ga), and the Pan-African Orogeny (0.65 – 0.55 Ga) (Goodwin,1996). All of these reddish sandstones are believed to have formed around the time of the Pan-African Orogeny.

Marten (1968) found the similarities between Luitikila formation in Chalabesa Mission area(1131NW) and Luapula Beds distributed in Mansa Region corresponding to northeastern part of Kundelungu formation. He thought that Luitikila formation correlated Luapula Beds through his detail observation of lithologies and sedimentary structures.

According to Cailteux(2005), Sedimentary age of Upper Kundelungu formation is 0.62 to 0.57Ga. The dating results of reddish sandstones in this study suggest that the Luitikila Formation corresponds with the Upper Kundelungu Formation.

Table 5.2.3.4-2 The Results of EPMA Dating Analysis (2)

Formation	Rock	Sample No.	Outcrop No.	UTM(N)	UTM(E)	Mineral	Age (100Ma)
Basement Complex (Granitoid)	Granite	RA006D	Pg70	8,829,974	249,107	Monazite	20.0±0.2 ～ 17.5±0.5
						Zircon	29.4±2.1 ～ 18.5±2.0
Katanga Supergroup (Luitikila Formation)	Sandstone	Dh-01	Lh7103102	8,789,966	280,299	Monazite	19.0±0.3 ～ 9.3±1.9
						Zircon	24.8±3.3 ～ 6.5±0.3
	Sandstone	DI-01	LI07101501	8,810,917	250,370	Monazite	10.4±1.8 ～ 6.3±0.8
						Zircon	21.5±2.7 ～ 7.6±1.3

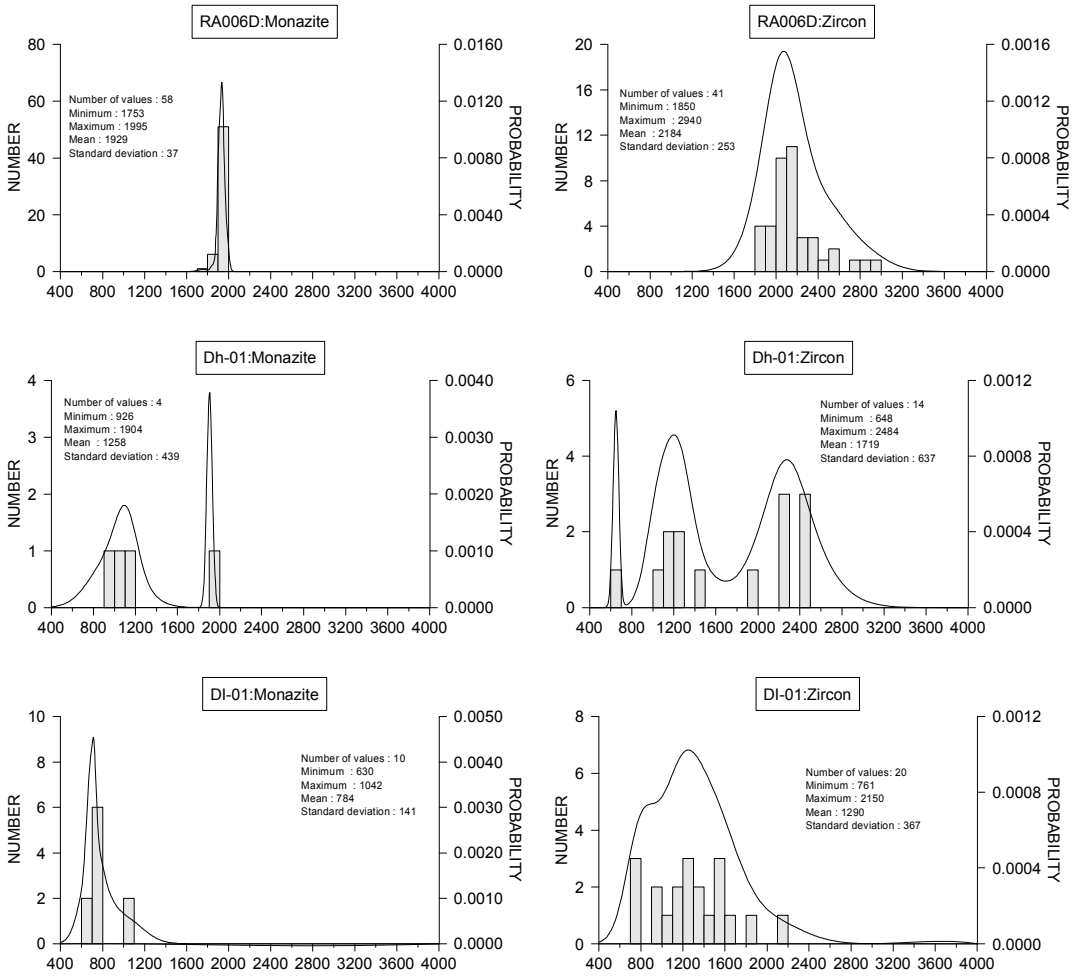

Fig 5.2.3.4-3 U-Th-Pb Monazite Ages and Zircon Ages of Samples in 1030SE Sheet area.

(3)1130NE Sheet

The dating results of reddish sandstone of the Luitikila Formation sampled in the 1130 NE sheet area are shown in Table 5.2.3.4-3 and Fig. 5.2.3.4-4.

The results of dating of reddish sandstone from the Lubaleshi River (RC011D) indicated a wide range of zircon age of 2.62±0.71 to 1.05±0.14Ga. The youngest age of 1.05±0.14Ga suggests that this formation was deposited after 1.05±0.14Ga.

The dating results of reddish sandstones in the Chilufya area (1030SE) corresponding to the sedimentary rocks in this sheet area suggests that this formation was deposited after 0.63±0.03Ga.

The dating results of detrital monazites in sandstone from the Kopa area (1130SE) indicated that the sandstone was deformed around 0.54Ga because of the large differences in age and thorium content between the rim and core of the monazite.

Considering the continuity of this formation and dating results above, the sedimentary age of this formation appears to be from 0.63Ga to 5.4Ga.

Marten (1968) found similarities between the Luitikila Formation in the Chalabesa Mission area (1131NW) and the Luapula Beds distributed in the Mansa Region corresponding to the northeastern part of the Kundelungu Formation. He thought that the Luitikila Formation corresponded to the Luapula Beds through his detailed observation of lithologies and sedimentary structures.

According to Cailteux (2005), the sedimentary age of the Upper Kundelungu Formation is 0.62 to 0.57Ga. The dating results of the Luitikila Formation in this study suggest that the Luitikila Formation corresponding to the Upper Kundelungu Formation.

Table 5.2.3.4-3 The Results of EPMA Dating Analysis (3)

Formation	Rock	Sample No.	Outcrop No.	UTM(N)	UTM(E)	Mineral	Age (100Ma)
Katanga Supergroup (Luitikila Formation)	Sandstone	RC011D	FC090420	8,739,782	268,236	Zircon	26.2±7.1 ～ 10.5±1.4

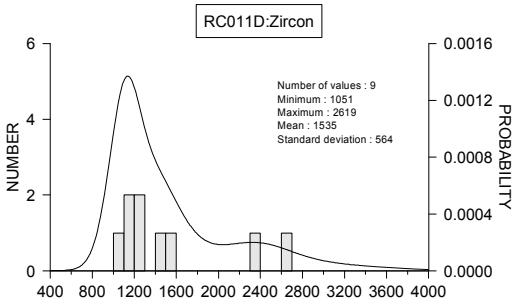

Fig 5.2.3.4-4 U-Th-Pb Zircon Ages of Samples in 1130NE Sheet area.

(4) 1130SE Sheet

The dating results of sandstone and siltstone of the Luitikila Formation sampled in the 1130 SE sheet area are shown in Table 5.2.3.4-4 and Fig. 5.2.3.4-5.

The results of dating of sandstone from the Luangoshi River (RC003D) indicated a wide range of monazite age from 1.97±0.02 to 0.52±0.09Ga. The detrital monazite was much younger age in the rim part (0.54Ga) than in the core part (1.92-1.96Ga) with a compositional difference that was observable under an electron microscope (Fig.5.2.3.4-5). Low thorium content in the rim part suggests that this rock was deformed around 0.54Ga. On the other hand, the detrital zircon age showed a wide range of 3.54±0.58 to 1.94±0.26Ga.

The results of dating of micaceous siltstone from the Luitikila River (RR002D) indicated a wide range of zircon age from 2.50±0.34 to 1.06±0.19Ga. No monazite was detected. The peak of probability distribution of zircon ages at around 1.1-1.2Ga corresponds to the period of Irumide Orogeny (1.35-1.10Ga).

Based on the dating results above, the sedimentary age is probably younger than Irumide Orogeny and older than the 0.54 Ga metamorphic age because the origin of sedimentary rock would be clastics of the basement complex or Irumide belt rocks.

Marten (1968) found similarities between the Luitikila Formation in the Chalabesa Mission area (1131NW) and the Luapula Beds distributed in the Mansa Region, corresponding to the northeastern part of the Kundelungu Formation. He thought that the Luitikila Formation correlated with the Luapula Beds through his detailed observations of lithologies and sedimentary structures.

According to Cailteux (2005), the sedimentary age of the Upper Kundelungu Formation is 0.62 to 0.57Ga. The dating results of the Luitikila Formation in this study suggest that the Luitikila Formation correlates with the Upper Kundelungu Formation.

Table 5.2.3.4-4 The Results of EPMA Dating Analysis (4)

Formation	Rock	Sample No.	Outcrop No.	UTM(N)	UTM(E)	Mineral	Age (100Ma)
Katanga Supergroup (Luitikila Formation)	Sandstone	RC003D	FC20080803	8,691,312	267,348	Monazite	19.7±0.2 ～ 5.2±0.9
						Zircon	35.4±5.8 ～ 19.4±2.6
	Sandstone	RB002D	N081101	8,689,786	253,786	Zircon	25.0±3.4 ～ 10.6±1.9

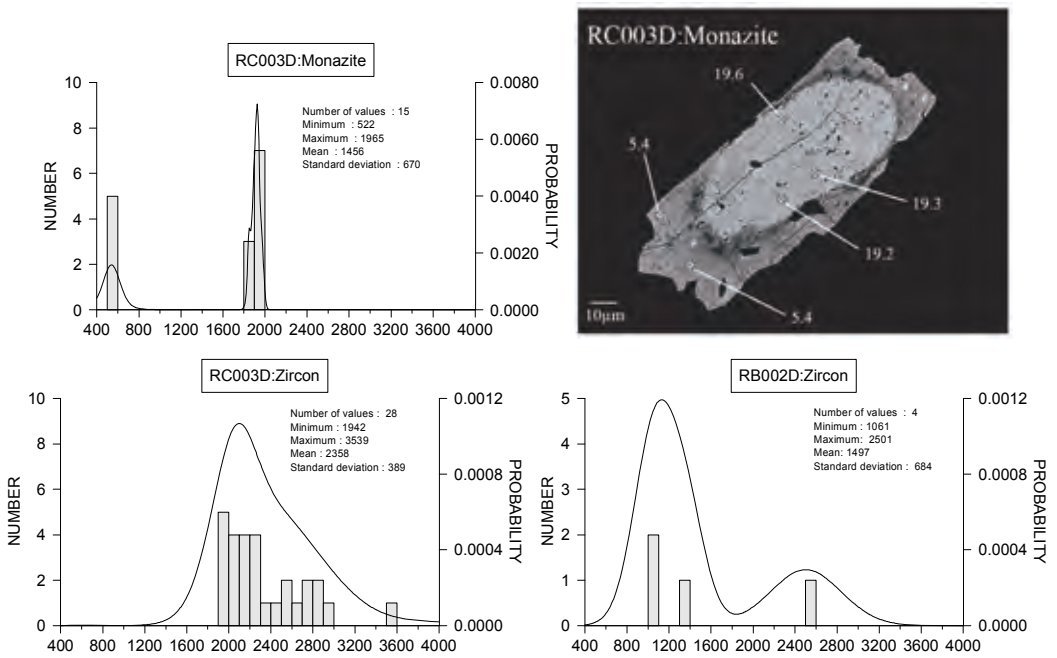

Fig 5.2.3.4-5 U-Th-Pb Monazite Ages and Zircon Ages of Samples in 1130SE Sheet area and electronic microscopic photo with dating results(100Ma) of detrital Monazite of RC003.

5.2.4 Geochemical Survey

5.2.4.1 Stream sediments geochemical survey

(1) Sampling

A total of 345 stream sediments were collected as geochemical samples during the geological survey. These samples were collected in the lowermost point of a primary stream or stream which drains a 10km2 catchment area. The UTM coordinates of all sample points were determined by handheld GPS receiver using Arc 1950 datum. Field information (coordinates, topography, features of collected materials) were recorded in "stream sediments sampling sheet" format (Appendix V-12). To avoid biases caused by grain size variability, all samples were sieved under 100mesh and over 150mesh. The samples that exceeded 100mesh were stored at GSD as archives. Fig. 5.2.4.1-1 shows sample localities of stream sediment geochemistry.

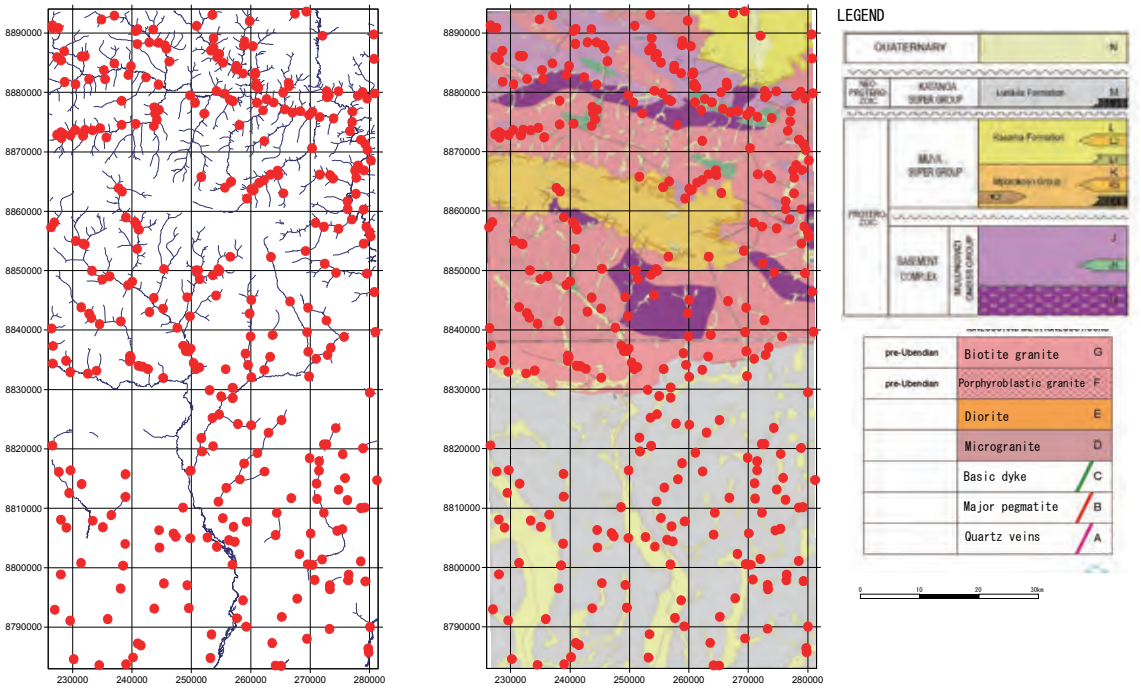

Fig. 5.2.4.1-1 Location of stream sediment sampling

(2) Assay

The assay analysis was carried out at ALS Chemex Lab in Canada. The 49 elements shown in Table 5.2.4.1-1 were analyzed.

The samples were pulverized to under 75 micro meters and digested by four-acid solvent (HF, HNO3, HClO4, HCl) in the laboratory. ICP-MS/ICP-AES and fire assay (for only Au) methods conducted for assay quantification. Detection limits of the assays are shown in Table 5.2.4.1-1. The

results of all assays are shown in Appendix V-13.

Table 5.2.4.1-1 Method and Detection Limit of Geochemistry

Element	Method	Detection Limit	Element	Method	Detection Limit
Ag	ICP-MS/ICP-AES	0.01 ppm	Na	ICP-MS/ICP-AES	0.01 %
Al	ICP-MS/ICP-AES	0.01 %	Nb	ICP-MS/ICP-AES	0.05 ppm
As	ICP-MS/ICP-AES	0.2 ppm	Ni	ICP-MS/ICP-AES	0.2 ppm
Ba	ICP-MS/ICP-AES	10 ppm	P	ICP-MS/ICP-AES	10 ppm
Be	ICP-MS/ICP-AES	0.05 ppm	Pb	ICP-MS/ICP-AES	0.2 ppm
Bi	ICP-MS/ICP-AES	0.01 ppm	Rb	ICP-MS/ICP-AES	0.1 ppm
Ca	ICP-MS/ICP-AES	0.01 %	Re	ICP-MS/ICP-AES	0.001 ppm
Cd	ICP-MS/ICP-AES	0.01 ppm	S	ICP-MS/ICP-AES	0.01 %
Ce	ICP-MS/ICP-AES	0.02 ppm	Sb	ICP-MS/ICP-AES	0.05 ppm
Co	ICP-MS/ICP-AES	0.1 ppm	Sc	ICP-MS/ICP-AES	0.1 ppm
Cr	ICP-MS/ICP-AES	1 ppm	Se	ICP-MS/ICP-AES	0.2 ppm
Cs	ICP-MS/ICP-AES	0.05 ppm	Sn	ICP-MS/ICP-AES	0.2 ppm
Cu	ICP-MS/ICP-AES	0.2 ppm	Sr	ICP-MS/ICP-AES	0.2 ppm
Fe	ICP-MS/ICP-AES	0.01%	Ta	ICP-MS/ICP-AES	0.01 ppm
Ga	ICP-MS/ICP-AES	0.05 ppm	Te	ICP-MS/ICP-AES	0.01 ppm
Ge	ICP-MS/ICP-AES	0.05 ppm	Th	ICP-MS/ICP-AES	0.2 ppm
Hf	ICP-MS/ICP-AES	0.02 ppm	Ti	ICP-MS/ICP-AES	0.005 %
In	ICP-MS/ICP-AES	0.005 ppm	Tl	ICP-MS/ICP-AES	0.02 ppm
K	ICP-MS/ICP-AES	0.01 %	U	ICP-MS/ICP-AES	0.05 ppm
La	ICP-MS/ICP-AES	0.2 ppm	V	ICP-MS/ICP-AES	1 ppm
Li	ICP-MS/ICP-AES	0.1 ppm	W	ICP-MS/ICP-AES	0.05 ppm
Mg	ICP-MS/ICP-AES	0.01 %	Y	ICP-MS/ICP-AES	0.05 ppm
Mn	ICP-MS/ICP-AES	5 ppm	Zn	ICP-MS/ICP-AES	2 ppm
Mo	ICP-MS/ICP-AES	0.05 ppm	Zr	ICP-MS/ICP-AES	0.5 ppm
Au	ICP-AES and Fire assay	0.001 ppm			

ICP: inductively coupled
ICP-MS/ICP-AES: Using both ICP-MS and ICP-AES

(3) Results

Descriptive statistics of all elements are shown in Table 5.2.4.1-2, histograms and cumulative frequency plots are shown in Appendix V-14, and geochemical distribution maps are shown in Appendix V-15.

Thirteen (Ba, Bi, Cs, Hf, K, Na, Pb, Rb, Sr, Te, Th, Tl, Zr) of the 49 elements tended to have higher values in the northern part of the sampled area (approximately located within in the 1030NE sheet area) than in the southern part (1030SE sheet area), whereas six (Au, Cr, Cu, P, Sb, Y) of the 49 elements tended to show higher values in the southern part. This geochemical contrast is concordant with the lithological distribution in which the basement complex is exposed in mainly the 1030NE sheet area and the Luilikila Fromation is exposed in mainly the 1030SE sheet area. Geochemical distribution maps for Au, Cu and Co are shown in Fig. 5.2.4.1-2.

Table 5.2.4.1-2 Descriptive statistics of stream sediment samples

element	unit	Min	Max	Mean	Range	Median	Mode	Standard Deviation (Stdv)	Variance (V)	Kurtosis	Skewness	Number of Samples (N)
Au	ppm	0.0005	0.015	0.0017	0.0145	0.001	0.0005	0.0019	0.0000	12.40	3.03	345
Ag	ppm	0.005	0.88	0.067	0.875	0.04	0.02	0.086	0.007	25.81	3.87	345
Al	%	0.29	11.85	2.561	11.56	1.69	0.87	2.196	4.822	1.70	1.39	345
As	ppm	0.1	58.8	2.32	58.7	0.9	0.1	6.70	44.90	49.65	6.82	345
Ba	ppm	20	710	172	690	130	70	133	17750	1.69	1.41	345
Be	ppm	0.025	25	2.501	24.975	1.23	0.25	3.333	11.106	10.71	2.82	345
Bi	ppm	0.02	1.2	0.190	1.18	0.15	0.12	0.150	0.023	9.61	2.54	345
Ca	%	0.01	0.89	0.056	0.88	0.03	0.01	0.088	0.008	32.66	4.87	345
Cd	ppm	0.01	0.5	0.039	0.49	0.02	0.01	0.056	0.003	18.76	3.60	345
Ce	ppm	7.73	500	68.894	492.27	49.9	18.55	62.563	3914.17	11.31	2.62	345
Co	ppm	0.1	56.3	5.45	56.2	2.8	0.7	7.85	61.62	15.58	3.52	345
Cr	ppm	2	94	17.6	92	12	6	14.5	210.6	2.46	1.42	345
Cs	ppm	0.3	23.6	3.320	23.3	1.82	0.79	3.528	12.449	5.56	2.17	345
Cu	ppm	0.9	79.9	13.44	79	7	2.5	15.15	229.42	4.10	1.98	345
Fe	%	0.05	26.6	1.255	26.55	0.44	0.21	2.702	7.303	37.26	5.43	345
Ga	ppm	0.87	31.3	6.598	30.43	4.2	13	5.714	32.655	1.90	1.45	345
Ge	ppm	0.025	0.64	0.078	0.615	0.06	0.025	0.072	0.005	12.06	2.67	345
Hf	ppm	0.3	15.8	2.78	15.5	2.6	2.6	1.60	2.57	13.63	2.42	345
In	ppm	0.0025	0.081	0.0229	0.0785	0.017	0.008	0.0168	0.0003	0.44	1.05	345
K	%	0.02	2.07	0.384	2.05	0.25	0.06	0.358	0.129	2.11	1.43	345
La	ppm	3.1	319	31.13	315.9	22	10.9	31.30	979.72	25.79	3.93	345
Li	ppm	0.5	91.8	10.87	91.3	6.1	2.7	12.54	157.22	11.00	2.77	345
Mg	%	0.005	0.18	0.037	0.175	0.03	0.01	0.030	0.001	3.53	1.73	345
Mn	ppm	7	2600	136.3	2593	90	38	191.0	36478.9	83.11	7.42	345
Mo	ppm	0.05	1.39	0.337	1.34	0.28	0.08	0.232	0.054	2.23	1.41	345
Na	%	0.005	1.73	0.060	1.725	0.02	0.01	0.165	0.027	58.89	7.11	345
Nb	ppm	1.4	61.4	14.48	60	10.7	3.9	10.67	113.94	1.13	1.17	345
Ni	ppm	0.8	115.5	11.48	114.7	6.4	1.4	13.38	178.91	13.37	2.79	345
P	ppm	20	2630	372	2610	160	50	465	215874	3.98	1.97	345
Pb	ppm	2.1	99.4	16.36	97.3	12	6.3	14.27	203.76	7.68	2.39	345
Rb	ppm	1.4	154.5	30.18	153.1	19.8	6.6	29.91	894.66	3.24	1.79	345
Re	ppm	0.001	0.002	0.0010	0.001	0.001	0.001	0.0001	0.0000	64.97	8.16	345
S	%	0.005	1.8	0.045	1.795	0.01	0.005	0.168	0.028	67.15	7.64	345
Sb	ppm	0.025	0.86	0.177	0.835	0.12	0.025	0.149	0.022	2.51	1.53	345
Sc	ppm	0.8	16.8	4.54	16	3.2	1.7	3.45	11.87	0.69	1.17	345
Se	ppm	0.5	5	2.0	4.5	2	2	0.8	0.6	2.16	0.94	345
Sn	ppm	0.1	4.2	1.21	4.1	0.8	0.5	0.94	0.89	0.56	1.17	345
Sr	ppm	1.1	59.1	11.90	58	9	6.2	9.54	91.04	3.38	1.69	345
Ta	ppm	0.06	13.9	1.148	13.84	0.84	0.5	1.287	1.656	40.40	5.20	345
Te	ppm	0.025	0.08	0.028	0.055	0.025	0.025	0.010	0.000	10.30	3.35	345
Th	ppm	1.1	145	10.19	143.9	7.7	5.2	11.45	131.07	69.22	7.06	345
Ti	%	0.022	0.673	0.2032	0.651	0.174	0.146	0.1220	0.0149	0.77	1.03	345
Tl	ppm	0.02	1.55	0.286	1.53	0.19	0.12	0.261	0.068	4.55	1.98	345
U	ppm	0.3	13.4	2.80	13.1	2	1.2	2.38	5.66	4.57	1.99	345
V	ppm	2	111	21.8	109	15	5	19.8	391.0	3.20	1.69	345
W	ppm	0.1	5.1	1.16	5	0.9	0.5	0.84	0.71	2.96	1.63	345
Y	ppm	1.7	107	17.97	105.3	11.4	4.7	17.74	314.72	5.77	2.16	345
Zn	ppm	1	282	25.0	281	14	6	30.0	898.8	19.26	3.46	345
Zr	ppm	9.8	482	91.28	472.2	81.8	137.5	53.07	2816.20	11.08	2.26	345

Assay results under detection limits have been replaced by 1/2 of the limits in the statistical analysis

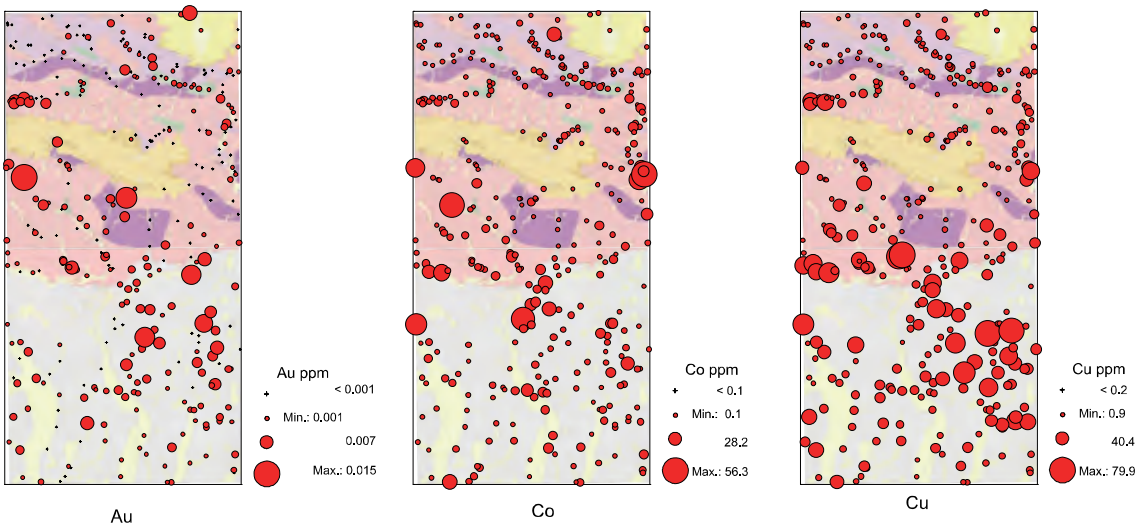

Fig5.2.4.1-2 Distribution of Stream Sediment Geochemistry (Au, Co, Cu)

As mentioned above, Cu showed higher values in the area of the Luitikila Formation and especially high values in the north-eastern part of the 1030SE sheet area. The north-eastern part of the 1030SE sheet area corresponds to the lowest horizon of the Luitikila Formation, which is comparable to the Cu-hosting Katanga Formation in the Zambian Copper Belt. However, at the present moment, the stratigraphic relation between the Luitikila Formation of the survey area and the Katanga Formation of the Copper Belt is uncertain because of poor exposure of this area. Au distribution indicates a higher value in the north-eastern part of the 1030SE sheet area and adjacent area of the basal horizon of the Mporokoso Group. There is no distinct trend in Co distribution.

5.2.4.2 Soil geochemical survey

A soil geochemical survey was conducted in the 1130NE and 1130SE sheet areas instead of a stream sediment geochemical survey because there were only a very few collectable points for stream sediments due to the extremely low topographic profile of this area. An additional soil geochemical survey was conducted in the 1030SE sheet area where a magnetic anomaly was detected by a previous GSD air-borne survey.

(1) Sampling

The sampling plan for soil geochemistry was set as a grid design with N-S intervals of 2 km and E-W intervals of 4 km. The alluvial plain which widely covers the western part of the 1130SE sheet area and the national park area were excluded from sampling targets. In cases where planned points occurred in cultivated fields, residential areas or alluvial cover, the points were re-set to uncontaminated ground.

Additional soil samples from the 1030SE sheet area were collected at three survey lines in

principally 500m point intervals. 500g of soil materials were collected from the so-called “B” horizon of soil profiles deeper than 50cm below the surface (Fig. 5.2.4.2-1). Plant fragments and pebbles were removed in the field. UTM coordinates of all sample points were determined by handheld GPS receiver using Arc 1950 datum. Field information (coordinates, topography, soil color and other features of collected materials or points) were recorded in “soil sampling sheet” format (Fig. 5.2.4.2-2). The sample ID ticket was separated from the sheet format and put into sample bags to prevent mix-ups of samples. A list of soil samples is shown in Appendix V-16.

Fig.5.2.4.2-1 Schematic soil profile

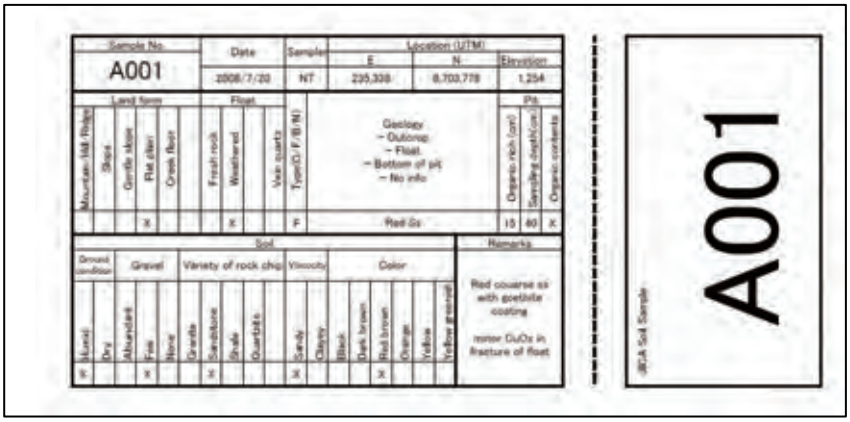

Fig. 5.2.4.2-2 Example of “soil sampling sheet” format

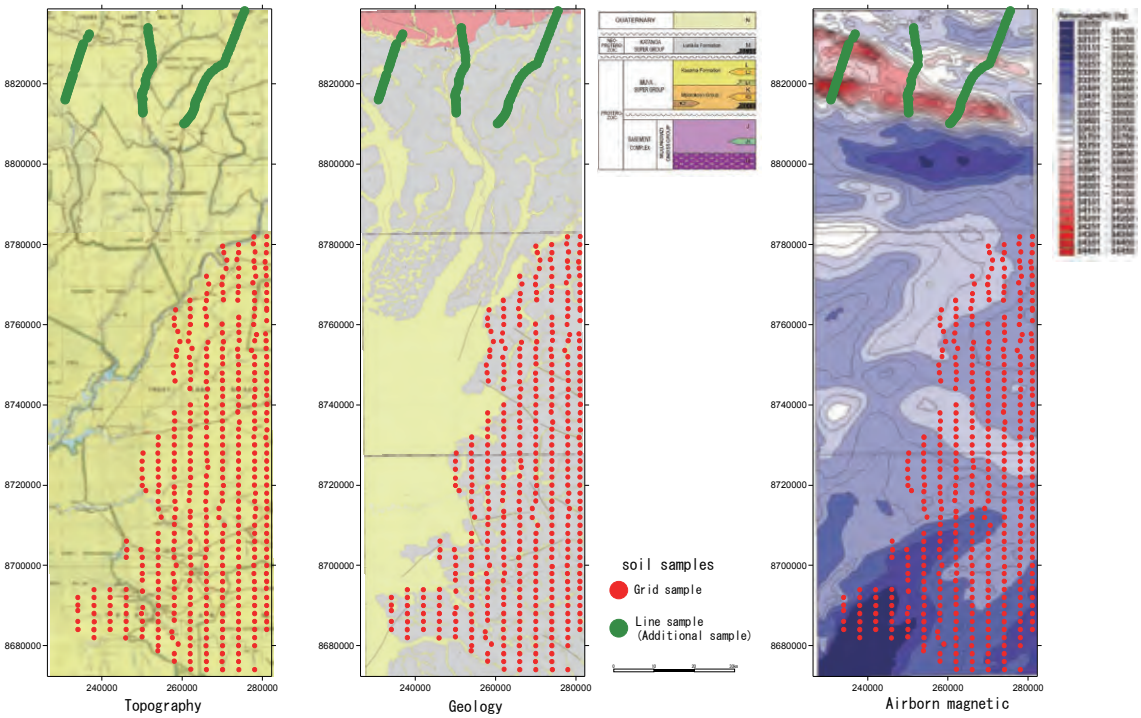

Fig. 5.2.4.2-3 Locations of soil geochemical sampling

(2) Assay

The assay analysis was carried out at ALS Chemex Lab in Canada. The following 49 elements as same stream sediments geochemistry shown in Table 5.2.4.1-1 were analyzed:

The samples were digested by four-acid solvent (HF, HNO3, HClO4, HCl) in the laboratory. ICP-MS/ICP-AES and fire assay (for only Au) were conducted for assay quantification. Detection limits of the assay are shown in Table 5.2.4.1-1. The results of all assays are shown in Appendix V-17.

(3) Results

Descriptive statistics of all elements are shown in Table 5.2.4.2-2, histogram and cumulative frequency plots are shown in Appendix V-18, and geochemical distribution maps are shown in Appendix V-19.

Of the 49 elements examined from grid samples (1130NE and 1130SE sheet areas), 38 (Ag, As, Ba, Be, Bi, Ca, Ce, Co, Cr, Cs, Cu, Fe, Ga, Ge, Hf, In, K, La, Li, Mg, Mn, Mo, Na, Ni, P, Pb, Rb, S, Sb, Sc, Th, Ti, Tl, U, V, Y, Zn, Zr)tended to have slightly higher values in the southern part of the 1130SE sheet area. A similar tendency was found in the line samples from the northern part of the 1030SE sheet area. It appears that these geochemical distributions are the result of lithology of the bed rock.

Geochemical distribution maps for Au, Co and Cu are shown in Figs. 5.3.4.2-4. There are no distinct geochemical anomalies and all elements show a relatively low value in comparison with the “Clark number”. No anomaly was found in the three sample lines located in the 1030SE sheet although Co and Cu mineralization had been expected based on the results of airborne magnetic anomaly in that area.

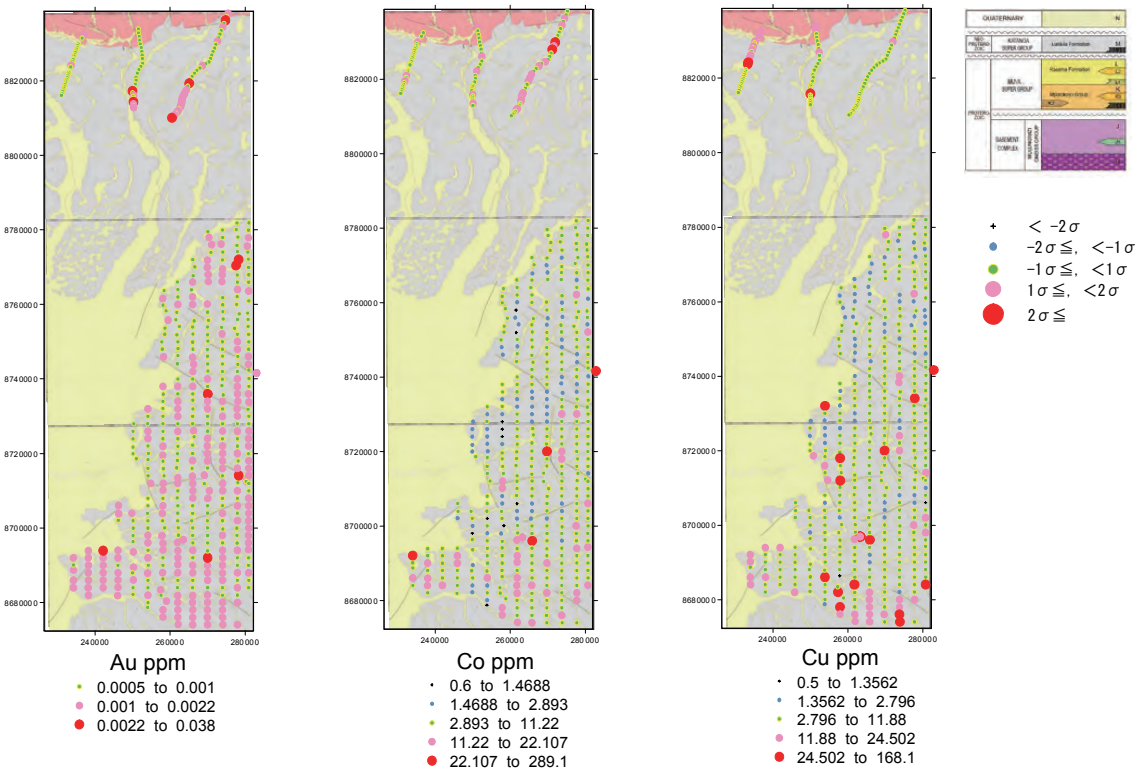

Fig. 5.2.4.2-4 Distribution of Soil Geochemistry (Au, Co, Cu)

Table 5.2.4.2-2 Descriptive statistics of soil samples

element	unit	Mini	Max	Mean	Range	Median	Mode	Standard Deviation (Stdv)	Variance (V)	Kurtosis	Skewness	Number of Samples (N)
Au	ppm	0.0005	0.038	0.0010	0.0375	0.0005	0.0005	0.0021	0.0000	202.03	12.96	539
Ag	ppm	0.005	0.46	0.031	0.455	0.02	0.005	0.033	0.001	51.27	4.84	539
Al	%	0.44	9.79	3.379	9.35	3.34	2.6	1.535	2.356	1.37	0.84	539
As	ppm	0.1	82	2.80	81.9	1.5	1.2	6.69	44.76	63.73	7.43	539
Ba	ppm	10	450	66	440	40	30	67	4453	8.34	2.59	539
Be	ppm	0.025	2.59	0.439	2.565	0.33	0.28	0.361	0.130	7.28	2.40	539
Bi	ppm	0.04	4.64	0.207	4.6	0.14	0.11	0.352	0.124	105.27	9.39	539
Ca	%	0.005	0.1	0.013	0.095	0.01	0.01	0.011	0.000	11.50	2.76	539
Cd	ppm	0.01	0.09	0.011	0.08	0.01	0.01	0.006	0.000	82.09	7.66	539
Ce	ppm	9.9	500	42.446	490.1	38	35	25.488	649.62	192.91	11.03	539
Co	ppm	0.6	289	7.81	288.4	5.8	4.6	16.80	282.30	232.52	14.71	539
Cr	ppm	4	334	25.4	330	19	15	31.9	1016.8	49.78	6.59	539
Cs	ppm	0.29	13.15	2.474	12.86	1.99	1.86	1.800	3.241	7.40	2.31	539
Cu	ppm	0.5	168	8.13	167.5	5.2	3.5	12.14	147.40	88.79	8.20	539
Fe	%	0.08	28.8	1.241	28.72	0.78	0.77	2.342	5.484	61.88	7.24	539
Ga	ppm	1.47	34.4	8.919	32.93	8.35	12.75	4.221	17.816	3.49	1.33	539
Ge	ppm	0.025	0.42	0.066	0.395	0.06	0.06	0.036	0.001	26.93	3.57	539
Hf	ppm	1	6.9	2.94	5.9	2.9	2.7	0.91	0.83	1.19	0.67	539
In	ppm	0.0025	0.245	0.0274	0.2425	0.024	0.022	0.0181	0.0003	46.84	5.05	539
K	%	0.01	1.25	0.216	1.24	0.13	0.12	0.217	0.047	3.83	1.92	539
La	ppm	4.1	42.2	16.85	38.1	15.8	14.4	6.32	39.93	1.55	1.03	539
Li	ppm	1.6	28.5	5.07	26.9	3.5	3.1	4.01	16.12	7.44	2.52	539
Mg	%	0.01	0.34	0.055	0.33	0.04	0.03	0.050	0.003	5.36	2.15	539
Mn	ppm	7	1390	60.4	1383	35	20	81.2	6594.4	134.24	8.93	539
Mo	ppm	0.025	5.56	0.628	5.535	0.5	0.29	0.580	0.336	25.94	4.24	539
Na	%	0.005	0.1	0.008	0.095	0.005	0.005	0.008	0.000	77.12	7.77	539
Nb	ppm	3	54	13.65	51	10.8	10.8	8.94	79.95	4.87	2.14	539
Ni	ppm	1.2	36.7	8.76	35.5	7.3	4.4	5.49	30.13	4.16	1.82	539
P	ppm	30	770	109	740	90	100	79	6166	33.26	4.93	539
Pb	ppm	2.7	790	12.77	787.3	9.6	8.7	37.33	1393.19	365.34	18.44	539
Rb	ppm	1.3	89.9	23.66	88.6	17.9	17.5	18.22	332.09	0.99	1.17	539
Re	ppm	0.001	0.016	0.0011	0.015	0.001	0.001	0.0007	0.0000	463.34	20.85	539
S	%	0.005	0.01	0.005	0.005	0.005	0.005	0.001	0.000	18.66	4.54	539
Sb	ppm	0.14	5.34	0.633	5.2	0.54	0.51	0.483	0.234	37.42	5.29	539
Sc	ppm	1.1	19.9	5.30	18.8	4.7	4.5	2.68	7.17	3.84	1.59	539
Se	ppm	0.5	3	1.6	2.5	2	2	0.5	0.3	-1.36	-0.14	539
Sn	ppm	0.4	5.9	1.97	5.5	1.9	1.9	0.79	0.62	2.10	1.06	539
Sr	ppm	1.5	18.9	6.19	17.4	5.7	5.1	2.56	6.57	3.24	1.44	539
Ta	ppm	0.21	28.6	1.494	28.39	1.24	0.84	1.396	1.950	264.47	13.90	539
Te	ppm	0.025	0.34	0.033	0.315	0.025	0.025	0.033	0.001	51.95	6.84	539
Th	ppm	2.2	30.4	8.22	28.2	7.8	8.2	3.21	10.31	5.51	1.57	539
Ti	%	0.074	0.631	0.2521	0.557	0.238	0.204	0.0853	0.0073	1.54	0.97	539
Tl	ppm	0.02	0.79	0.220	0.77	0.18	0.15	0.140	0.020	1.06	1.08	539
U	ppm	0.5	7.3	1.38	6.8	1.2	0.9	0.74	0.54	20.19	3.71	539
V	ppm	6	438	36.6	432	27	25	42.9	1840.3	45.92	6.24	539
W	ppm	0.4	2140	45.09	2139.6	29.1	0.9	99.06	9812.35	373.26	17.78	539
Y	ppm	0.5	25.9	9.14	25.4	8.5	6.9	3.85	14.80	1.72	1.16	539
Zn	ppm	1	61	12.4	60	10	8	8.4	70.1	3.65	1.69	539
Zr	ppm	31.2	233	96.08	201.8	93.3	101.5	32.07	1028.46	1.56	0.87	539

Assay results under detection limits have been replaced by 1/2 of the limits in the statistical analysis

5.2.5 Summary of mineralization

5.2.5.1 Stratigraphy, geochronology and comparison with the Copperbelt area

This survey confirmed that the area is underlain by 1) Basement complex, 2) Muva super group, 3) Katanga super group and 4) Quaternary deposits. EPMA dating analysis indicates that the metamorphosed age of the basement complex is 1.94 to 2.0 Ga. The Muva super group was affected by weak metamorphism at 1.1 Ga following the primary deposition at 1.74±0.14 Ga. These results are consistent with those of previous investigations (e.g. Daly and Unrug, 1982, De Waele and Fitzsimons, 2007 etc.).

Although no detailed geochronolgical information on the formation had previously been reported, the EPMA dating analysis shows that the deposition age of the Luitikila formation (Katanga super group) which distributes in the survey area is around 0.63±0.03 Ga. This age corresponds to the forming age of the Kundelungu Formation (upper part of the Katanga super group; Fig. 5.2.5-1) in the mineralized Copperbelt area. Cu mineralizations in the Copperbelt are mainly distributed in the Roan Formation (Lower part of Katanaga super group) as “strata bound” type deposits. No mineralization was reported in the Kundelungu formation ,equivalent of the Luitikila Formation. Therefore it is assumed that the Copperbelt type mineralization is not expected in the Katanaga Formation of the survey area.

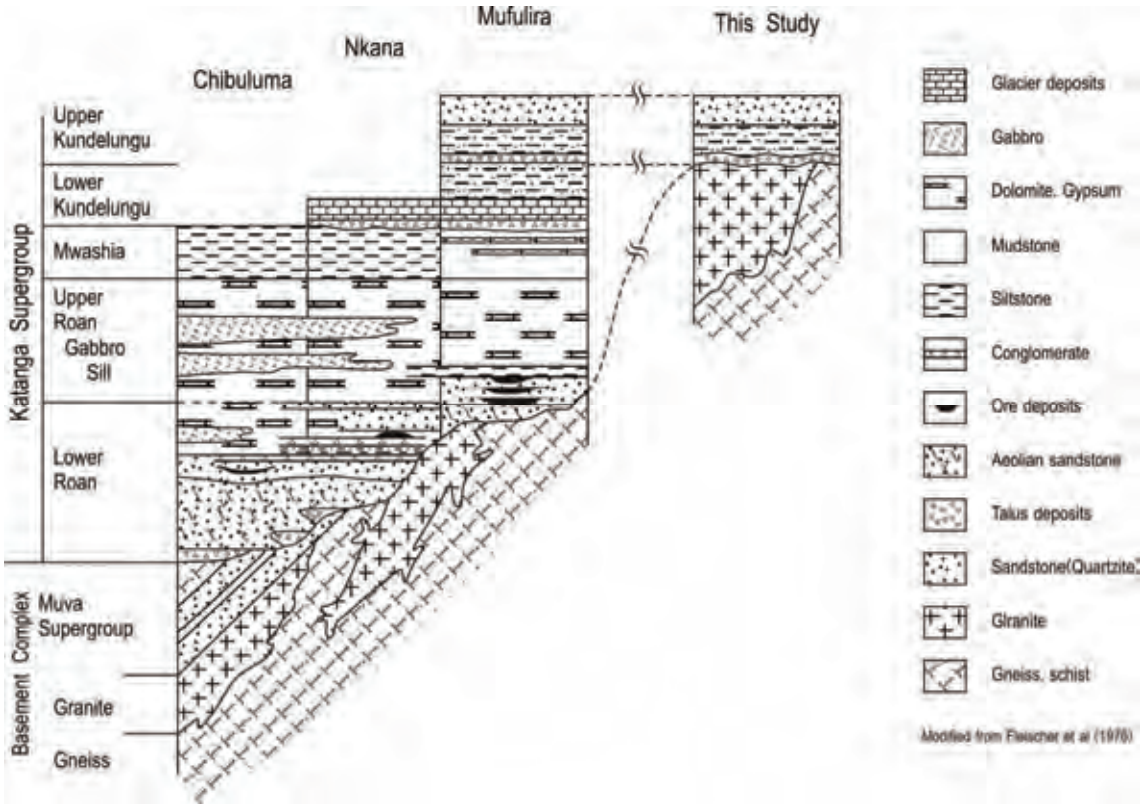

Fig 5.2.5-1 Schematic section of the Zambian Copper Belt Type Cu mineralization

5.2.5.2 Mineraliztion

(1) Cu, Co mineralization

The Cu values of soil samples in the area of Katanga Supergroup were rather low and there were no distinct geochemical anomalies, although a slightly higher tendency in Cu values was indicated by the results of the stream sediment samples in the area. “Copperbelt type” Cu mineralizations were expected in the basal horizon of Katanga Supergroup located in the 1030SE sheet area by the results of a previous airborne magnetic survey. However, no Cu or Co geochemical anomalies were found, even in the soil geochemical survey lines which had been set up so that they would intersect with magnetic anomalies. In addition, no significant Cu or Co mineralization was detected in this survey. It may be assumed that the low geochemical values are the result of strong weathering and leaching. The magnetic anomaly zone is still prospective because there are possibility of different type of mineralization expected subsurface of the anomaly.

It is recommended that detailed geological mapping, rock geochemistry and geophysical survey (especially “electromagnetic” methods) targeted in the magnetic anomaly be conducted to reveal the subsurface Cu and Co potential.

(2) Au mineralization

Exploration work that targeted Au mineralization in basal conglomerate of the Mporokoso Group was conducted to the north of this survey area (Kasama – Mbala area). Stream sediment geochemistry of this study shows weak Au anomalies around the basal horizon of the Mporokoso Group. It appears that the Au derived from the basal conglomerate of the Group. Detailed distribution of Au concentration in the Mporokoso Group was not revealed in this study because the rock geochemistry sampled from Mporokoso Group (RB018; Appendix V-10) showed a very low Au grade (<0.001 ppm).

It is recommended that a detailed survey, such as systematic rock geochemistry, be conducted to evaluate the Au potential in the Group.

(3) Silica stone deposits

In this study, whole rock analysis of quartzose sandstone or quartzite was conducted to evaluate the potentiality of the silica stone deposits (Appendix V-8). No sample exceed the required SiO_2 grades for Industrial applications such as metallic silicon material although these samples show relatively high SiO_2 values: 92.9% in quartzose sandstone of the Katanga Supergroup (RC003W), 96.9% in quartzite of the Mporokoso Group (RB011W) and 98.4% in quartzite of the Kasama Formation (RB015W). The quartzite of the Mporokoso Group and Kasama Formation tend to form mesa-like landforms because of its resistance to erosion.

It is recommended that a detailed survey and systematic assaying of quartzite be conducted to evaluate of the potential of industrial grade silica stone deposits in the area.

Table 5.2.5-1 Requirement quality of silica stones for Industrial applications

Application	SiO_2	Fe_2O_3	Al_2O_3	CaO	TiO_2	Others
Opaque quartz glass	>99.8%	<0.02%	<0.1%	<0.1%		
Optical lens	>99.5%	<0.02%	<0.05%			
Metallic silicon	>99.5%	<0.02%	<0.1%	<0.03%		
silicon carbide(carborundum)	>99.6%	<0.2%	<0.2%		<0.2%	
ferrosilicon	>97.0%		<0.7%		<0.03%	<P 0.1%
iron manufacturing material	>97.0%		<3.0%			<P 0.1%
Silica mortar	>93.0%	<1.5%	<3.0%			

References

1. Andrew-Speed, C.P.,1982. Senga PL 188 Quarterly Report No.1 for the Period Febrary-May 1982. Minex Department, Zimco Ltd.7pp
2. Cailteux JLH, Kampunzu AB, Lerouge C, Kaputo AK, Milesi JP (2005); Genesis of sediment-hosted stratiform copper–cobalt deposits, central African Copperbelt. J Afr Earth Sci 42:134–158
3. Daly M. C. and Unrug, R., 1982, The The Muva Supergroup, Northern Zambia: a craton to mobile belt sedimentary sequence, Transactions of the geological society of South Africa, 85, 155-165p.
4. De Waele, B. and Fitzsimons, I. C. W., 2004, The age and detrital fingerprint of the Muva Supergroup of Zambia: Molassic Deposition to the Southwest of the Ubendian Belt, Abst., Geoscience Africa, 2p.
5. De Waele, B, and Fitzsimons, I.C.W., 2007, The nature and timing of Palaeoproterozoic sedimentation at the southeastern margin of the Congo Craton; zircon U–Pb geochronology of plutonic, volcanic and clastic units in northern Zambia, Precambrian Research, 159, 95-116.
6. Drysdall, A. R., 1960, Geology and geomorphology of the Chishimba Falls, Kasama, Records of the Geological Survey Department, Northern Rhodesia for 1959, 30-34p.
7. Guernsey, T.D.,1941, Summary report on the Concession Areas of Loangwa Concession (N.R.) Limited and Rhodesia Minerals Concessions Limited.(Unpublished)
8. Marten, B.E., 1968, The geology of the Chalabesa Mission area; Explanation of degree sheet 1131, NW quarter. 23, Geological Survey Department of Zambia, Lusaka. 25p.
9. Maczka, L. and Cap, M., 1973, Brick-clays in the Kasama area, with particular reference to the Lukashaya, Economic report of the geological survey, No.43, Ministry of mines and mining development, Republic of Zambia,34p.
10. Sykes, J. M. D., 1995, The geology of the Chipili and Nsombo areas; Explanation of degree sheet 1029, SW and SE quarters. 72, Geological Survey Department of Zambia, Lusaka. 16p.
11. Thieme, J., G., 1970; The geology of the Mansa area; Explanation of degree sheet 1128 of NW and NE quarter. 26, Geological Survey Department of Zambia, Lusaka.13.
12. Unrug, R., 1982. The Kasama Formation: lithostratigraphy, palaeogeography and regional position, Palaeogeography of Zambia. Geological Society of Zambia, Lusaka, 8p.